R. & M. No. 3638

R. & M. No. 3638

MINISTRY OF TECHNOLOGY

AERONAUTICAL RESEARCH COUNCIL
REPORTS AND MEMORANDA

An Analysis of Oblique and Normal Detonation Waves

By L. H. TOWNEND
Aerodynamics Dept., R.A.E., Farnborough

LONDON: HER MAJESTY'S STATIONERY OFFICE
1970
PRICE £1 2*s* 0*d* [£1·10] NET

An Analysis of Oblique and Normal Detonation Waves

By L. H. Townend

Aerodynamics Dept., R.A.E., Farnborough

Reports and Memoranda No. 3638*

March, 1966

Summary.

Plane detonation waves are analysed, on the assumption that the ratio of specific heats and the molecular weight are constants. Heat release is quoted in terms of a dimensionless parameter F, such that, for Chapman-Jouguet detonations $F = 1$, for any strong detonation $1 < F < 2$, and for shock waves $F = 2$. Wave properties are shown to be functions either of heat release and the component of upstream Mach number normal to the wave, or of heat release and both normal and streamwise components of upstream Mach number. The expressions can be used to generalise existing R.A.E. computer programmes for flows with two-dimensional or axisymmetric shock waves; they thus allow computation of two-dimensional or axisymmetric flow fields formed between a body and a detonation wave.

LIST OF CONTENTS

*Replaces R.A.E. Technical Report No. 66 081—A.R.C. 28 317.

---

1. *Introduction.*

If a shock wave traverses a supersonic stream of pure gas, a rise in static temperature necessarily occurs; however, if real gas effects are negligible, then energy is neither lost nor gained and the stagnation temperature does not change. Conversely, in a flow of pre-mixed fuel and air (or of other gaseous or vaporised reactants) a shock wave may produce a rise in static temperature which exceeds that required for ignition of the mixture, and energy will then be released due to combustion of some or all of the fuel; the static temperature will be thereby increased still further, and the stagnation temperature at some station downstream will now be found to have risen. According to the distance between the shock and the flame front, such a process may be described as shock-induced combustion (in which combustion occurs some way downstream of the shock) or as a detonation wave (in which the effects of heat release act in full upon the shock).

Questions arising with regard to either type of reaction concern

1. the conditions (e.g. the pressure, temperature and velocity of the stream, and the nature of the reactants) for which an exothermic reaction can occur;
2. whether a detonation wave is ever obtained in practice, or merely forms a hypothetical limit to shock-induced combustion;
3. the manner in which such processes behave, and hence methods by which they may be controlled, and
4. the merits of such processes as practical means for the efficient release of heat to streams in which, initially or throughout the flow, velocities are required to be supersonic.

The present Report is mainly concerned with the third question, but the other questions receive some attention in Section 2; this comprises a brief survey of certain experimental studies, and of investigations into the performance and efficiency in practical applications of detonation waves or shock-induced combustion.

Nearly all these preliminary studies in fact relate to hypersonic ramjets in which heat addition is assumed to occur through a detonation wave. The performance of such engines should of course be assessed over appropriate ranges of Mach number and altitude, and in the context of relevant intake, nozzle and airframe designs; such an assessment should show how performance may be optimised (for example, by minimising specific fuel consumption or dissociation losses), and how such ramjets compare, in various types of mission, with optimised ramjets using other forms of heat release. The author does not know of any such published work. Even of papers which consider the behaviour of detonation waves in isolation, few have gone beyond a study of static pressure, density and temperature (and in some, of flow velocity and Mach number); furthermore, most analyses are restricted to normal waves. In the absence of more general analyses, a basic study of the general equations describing the detonation wave was thought to be justified.

This Report is concerned with the theoretical behaviour of the plane detonation wave which, from an initially uniform flow of pre-mixed combustible gases, produces a uniform flow of gaseous products of combustion, either aligned with or inclined to the upstream flow, depending on whether the wave itself is normal or oblique. In terms of heat release and the normal and streamwise components of upstream Mach number, the analysis deals with the following properties: the static pressure, density and temperature, stagnation pressure and temperature, entropy rise, wave angle and flow deflection, and normal and streamwise components of discharge Mach number and flow velocity. For normal and oblique waves it considers the general case of the strong detonation wave (in which the component of discharge Mach number normal to the wave is subsonic), and both limiting cases (i.e. the Chapman-Jouguet detonation, with which the flow is discharged at a velocity whose component normal to the wave is sonic, and the simple shock across which heat release is zero).

The effects of changes across a given wave in the ratio of the specific heats and in the molecular weight are not included.

2. *Brief Survey of Selected Experimental and Analytic Work.*

Since the earliest tests on gaseous detonation (by Berthelot and Vieille[1], and Mallard and Le Chatelier[2]), most experiments have also concerned waves which advance supersonically up tubes filled with pre-mixed reactants. If such waves are normal to their direction of motion, they would be expected to reach a stable velocity at the Chapman-Jouguet condition[3,4], at which the flow is discharged at sonic speed relative to the wave; however, actual tests on waves which move relative to their containers are complicated by wave/boundary layer interactions, and their velocities of propagation can be changed by experimental technique, for example, when the wave is 'driven' up the tube by means of a piston.

An alternative approach to the formation of moving waves was suggested in 1943 by Zeldovich and Leypunskiy[5], who proposed that combustion might be stabilised by the shock wave produced by a bullet fired through a combustible mixture; the earliest demonstration of this technique was by Zeldovich and Shlyapintokh[6], who reported preliminary tests in 1949. In 1960 experiments by Ruegg at the National Bureau of Standards[7] were described as having established laminar combustion behind the curved shock wave ahead of a spherical missile fired down a range at supersonic speed; similar tests by Ruegg and Dorsey were reported[8] in 1962 and comments on these tests have been made by Samozvantsev[9]. In 1964, tests of a similar type were reported by Behrens, Struth and Wecken[10], and further tests (in which the missiles were cone-cylinders) were described by Behrens and Struth[11]. At the present time, Peckham and Crane are experimenting with the missile technique at R.A.E., Farnborough (1966).

No tests on moving waves can easily allow protracted or instrumented measurements to be made. However, recent tests by Voytsekhovsky *et al*[12-15] and Nicholls *et al*[16,17] have yielded photographs of a type of detonation wave which stably performs continuous circuits of a circular channel. Also, as early as 1941, Hoffmann[18] was operating an engine in which an intermittent detonation wave was used for heat release and in 1952 Bitondo[19,20] Bollay[19,20] and Kendrick[20] described analyses of related phenomena; in 1957, Nicholls, Wilkinson and Morrison[21] reported analytic and experimental work on a pulsating detonation tube. At that time however a detonation wave had never been brought fully to rest under laboratory conditions.

The achievement of standing detonation waves was independently claimed, in 1958, by Nicholls *et al*[22] of Michigan University, and by Gross[23] of the Fairchild Engine Division, New York. Controversy regarding the nature of the combustion* which had been obtained[24-29] led to further experiments by Rubins *et al*[30-32], and by 1964, stable combustion had been produced behind stationary shock waves, both normal and oblique, in supersonic flows of high stagnation temperature. Rubins' experiments (and also those of Suttrop[33]) demonstrated shock-induced combustion, rather than standing detonation, since the reaction length was too great for the process to be regarded as a discontinuity: however, in some of Nicholls' experiments [22,24], combustion produced a change in wave position which was consistent with detonation at the Chapman-Jouguet condition. It seems that the achievement of true detonation waves must await experiments in which temperatures accelerate the kinetic reactions to such an extent that the wave may be regarded as a discontinuity; only under these circumstances could the classical detonation theory be appropriately compared with experimental results.

Much more detailed reviews of research on detonation waves have been presented in 1959 and 1963 by Oppenheim *et al*[34,35], and a review of Russian work in the period 1958–January 1964 has been published[36] by the Library of Congress, U.S.A. Some attention has also been given to the evaluation of detonation waves as practical processes for releasing heat in flows having stream velocities which, either initially or throughout the flow, are required to be supersonic. For example, Gross has suggested their use in chemical processing plants, and studies have been made of the theoretical performance of engines which use intermittent detonation[21], or waves which are stabilised[37-40], or magnetically excited[41], and of rockets based on rotating detonation waves[16,17]; a few investigations have also been made which are relevant[42-46] to the use of detonation waves, stabilised by unspecified means in the external flow beneath a body so as to produce upon it, by external combustion, a propulsive and/or a lifting force. For even more advanced propulsion systems, the study of detonation waves has been recommended[47] to assist in the eventual design of gaseous fission reactors and pulsed plasma accelerators.

Of analyses of detonation waves, most have been restricted (as mentioned in the Introduction) to a study of static pressure, density and temperature (and in some, of flow velocity and Mach number); in most of these analyses only normal waves were considered, but a few papers have dealt with plane, oblique detonation waves[48-52] and waves which occur at other than the Chapman-Jouguet condition[48-52]. Only two papers have dealt with the analysis of conical or other axisymmetric detonation waves[53,54] and of these, only the second[54] presents quantitative results. In view of this, a basic study of the general equations describing detonation waves was thought to be justified.

The analysis (presented in Sections 3 to 5 and Appendices A to C) is based on the fact that any detonation wave can be regarded as a member of a family of flows, of which all members act as discontinuities in supersonic streams of pre-mixed reactants. At one extreme, such waves correspond to Chapman-Jouguet detonations and at the other, to simple shock waves. Heat release is quoted in terms of a parameter F, such that for Chapman-Jouguet detonations $F = 1$, for strong detonations $1 < F < 2$, and for shock waves $F = 2$. This parameter was originally derived, for the particular case of normal waves, by Adamson and Morrison[55]; its use as above allows emphasis on the thermodynamic nature of a detonation wave, and has since been used by Bartlett[56] in computing the properties of conical detonations.

3. *Basic Equations for Supersonic Flow with Heat Release in an Inclined Plane.*

In Fig. 1a a sketch of the two-dimensional flow through a plane oblique detonation wave is shown. A uniform flow approaches the wave at velocity V_1 and is discharged at velocity V_2, the wave inclination and flow deflection being the acute angles ζ and δ respectively. Note that the sketch of Fig. 1a represents the flow through any region on a plane wave (as in Fig. 1b), but that it also represents the flow through

*At least some of Gross' original results were obtained under conditions in which combustion occurred upstream (at the fuel injector) and so acted as a 'pilot flame' for the main combustion region downstream of the shock wave. While such a process cannot be described as detonation, it forms an interesting variant of shock-induced combustion. Also, being subject to a so-called hysteresis effect (by which the combustion, once established, could be maintained at stagnation temperatures below those at which flame-out was expected), it might be particularly useful in stabilising combustion in hypersonic ramjets.

an elemental area of a non-planar wave, for example, one of those in Figs. c to e. R.A.E. computer programmes already exist[57,58] or are being developed[58] to calculate the flow through two-dimensional or axisymmetric shock waves, on which any longitudinal curvature is, as in Figs. 1 c to e, in the attenuating sense; the two-dimensional analysis which follows can be used to generalise these programmes and so allow computation of axisymmetric flow fields[56] formed between a body and a detonation wave.

If, in the flow of Fig. 1a the effects of dissociation and γ-variation are negligible, then the following equations apply:

$$\rho_1 u_1 = \rho_2 u_2 \tag{1}$$

$$p_1 + \rho_1 u_1^2 = p_2 + \rho_2 u_2^2 \tag{2}$$

$$v_1 = v_2 \tag{3}$$

$$\tfrac{1}{2}(u_1^2+v_1^2) + \frac{a_1^2}{\gamma-1} + q = \tfrac{1}{2}(u_2^2+v_2^2) + \frac{a_2^2}{\gamma-1} \tag{4}$$

$$a^2 = \gamma p/\rho = \gamma R T \tag{5}$$

$$\left.\begin{aligned} \frac{C_p}{C_v} &= \gamma \\ C_p - C_v &= R \end{aligned}\right\} \text{ Therefore } C_p = \frac{\gamma R}{\gamma-1}. \tag{6}$$

From equations (1), (2) and (5) it follows that

$$\gamma M_{N1}^2 \left(\frac{u_2}{u_1}\right)^2 - (1+\gamma M_{N1}^2)\left(\frac{u_2}{u_1}\right) + \left(\frac{a_2}{a_1}\right)^2 = 0. \tag{7}$$

From equations (3), (4), (5) and (6) it follows that

$$\left(\frac{u_2}{u_1}\right)^2 = 1 + \frac{2}{(\gamma-1) M_{N1}^2}\left(1 + \frac{q}{C_p T_1} - \left(\frac{a_2}{a_1}\right)^2\right). \tag{8}$$

If $\left(\frac{a_2}{a_1}\right)$ is eliminated between equations (7) and (8), the resulting quadratic equation in $\left(1-\frac{u_2}{u_1}\right)$ solves as

$$1-\frac{u_2}{u_1} = 1-\frac{\rho_1}{\rho_2} = \frac{M_{N1}^2-1}{M_{N1}^2(\gamma+1)}\left[1+\sqrt{1-\frac{2(\gamma+1)M_{N1}^2}{(M_{N1}^2-1)^2}\frac{q}{C_p T_1}}\right] \tag{9}$$

in which $q/C_p T_1$ ($\equiv$ Damköhler's second parameter) quotes the heat released per unit mass of fluid in terms of the upstream value of specific static enthalpy; note that the sign of the square root has been chosen to give, for a normal shock wave (i.e. for $u_1 = V_1, u_2 = V_2, q = 0$), the standard equation (e.g. equation (94) in Ref. 59):

$$\frac{u_2}{u_1} = \frac{\rho_1}{\rho_2} = \frac{V_2}{V_1} = \frac{2+(\gamma-1)M_1^2}{(\gamma+1)M_1^2} = \frac{1}{(M_1^*)^2}\left[\frac{V_1}{M_1^*} \equiv a_1^* \equiv \text{critical velocity of sound}\right].$$

For oblique or normal plane waves, equation (9) may be re-written as

$$M_{N1}^2\left(1-\frac{u_2}{u_1}\right) = M_{N1}^2\left(1-\frac{\rho_1}{\rho_2}\right) = \left(\frac{M_{N1}^2-1}{\gamma+1}\right)F, \text{ in which } F \equiv 1+\sqrt{1-\frac{2(\gamma+1)\,M_{N1}^2}{(M_{N1}^2-1)^2}\,\frac{q}{C_p\,T_1}}. \quad (10)$$

If only normal, plane waves are considered (i.e. $M_{N1} = M_1$), then in equation (10), F takes the form derived by Adamson and Morrison, who showed for these conditions that $F = 2$ for shock waves, $F = 1$ for Chapman-Jouguet detonation waves and, for any strong detonation wave, $1 < F < 2$.

As an alternative to the use of F, heat release may be quoted in terms of the upstream stagnation enthalpy ($C_p\,T_{T1}$), for example by use of a heat-release coefficient (as used by Weber[52])

$$C_q = q/C_p\,T_{T1} = q\bigg/\left[C_p\,T_1\left(1+\frac{\gamma-1}{2}M_1^2\right)\right]; \quad (11)$$

equation (10) then takes the form

$$M_{N1}^2\left(1-\frac{u_2}{u_1}\right) = M_{N1}^2\left(1-\frac{\rho_1}{\rho_2}\right) = \left(\frac{M_{N1}^2-1}{\gamma+1}\right)F,$$

$$F = 1+\sqrt{1-\frac{2(\gamma+1)\,M_{N1}^2}{(M_N^2-1)^2}\bigg/\left(1+\frac{\gamma-1}{2}M_1^2\right)C_q}$$

$$C_q = [1-(F-1)^2]\,\frac{(M_{N1}^2-1)^2}{2(\gamma+1)M_{N1}^2}\bigg/\left(1+\frac{\gamma-1}{2}M_1^2\right)$$

$$= \frac{F\,(2-F)\,(M_{N1}^2-1)^2}{2(\gamma+1)\,M_{N1}^2}\bigg/\left(1+\frac{\gamma-1}{2}M_1^2\right).$$

Equation (10) can then be written in the form given by Weber (*see* equation (7) of Ref. 52).

A choice between the various heat release parameters noted above is made in Section 3.1.

3.1. *Choice of a Heat Release Parameter.*

Heat release across oblique or normal detonation waves may be quoted as

(1) $q/C_p\,T_1$

or (2) $C_q = q/C_p\,T_{T1} = q\bigg/\left[C_p\,T_1\left(1+\frac{\gamma-1}{2}M_1^2\right)\right]$

or (3) $F = 1+\sqrt{1-\frac{2(\gamma+1)\,M_{N1}^2}{(M_{N1}^2-1)^2}\,\frac{q}{C_p\,T_1}}.$

The parameter $q/C_p\,T_1$ has been used in most of the literature, presumably because it occurs explicitly in some forms of the energy equation. However, in performance work on, for example, a hypersonic ramjet operating at a free-stream Mach number of M_∞ and using a detonation wave for heat release, the use of static enthalpy as a reference for q involves the need to specify the discharge Mach number of the associated intake $\left(\text{since for } T_{T1} = T_{T\infty}, \text{ it follows that } \frac{T_1}{T_\infty} = \frac{2+(\gamma-1)\,M_\infty^2}{2+(\gamma-1)\,M_1^2}\right)$. If allowance is made for varying the intake design, the reference temperature T_1 may change simultaneously; the merit of Weber's choice[52] of C_q is that, for flight at a given T_∞ and M_∞, and for an adiabatic intake process ($T_{T1} = T_{T\infty}$), heat release is quoted in terms of stagnation enthalpy ($C_p\, T_{T\infty}$) which is independent of both the extent and the efficiency of the intake compression.

Unfortunately, neither parameter gives a direct indication of the strength of the detonation, i.e. of its relationship to the limiting Chapman-Jouguet or shock wave conditions. To achieve such an indication for normal waves, Adamson and Morrison[55] proposed the use of F ($1 \leqslant F < 2$ for all possible thermodynamic types of detonation wave). In this Report, F has been shown to be applicable to both normal and oblique waves; since, in performance work, its adoption does not prevent simultaneous reference to free-stream conditions, it is used throughout this Report for quoting heat release.

4. *Presentation of Results.*

It is found that properties of detonation waves are functions either $f(F, \gamma, M_{N1})$ or $f(F, \gamma, M_{N1}, M_1)$. Expressions of the first type are considered in Section 5.1 (and Appendix A), and those containing terms in M_1 are considered in Section 5.2 (and Appendices B and C). Principal expressions are listed in Table 1, but instead of providing working charts for particular values of γ, F etc, the forms which such charts would take are illustrated diagrammatically in Figs. 2 to 13. Data which describe particular wave conditions (for example maximum flow deflection through waves at constant γ) are listed in Tables 2 to 5, and more data, from which working charts could be accurately plotted, are presented in Table 6; this last Table can be obtained separately[60], by application to R.A.E., Farnborough and presents data for Chapman-Jouguet detonations for $\gamma = 1{\cdot}4$ and Mach numbers in the ranges $1{\cdot}5 \leqslant M_{N1} \leqslant 6$, $M_{N1} \leqslant M_1 \leqslant 15$. Atlas and Mercury computer programmes for Tables 2 to 6 (all written by Mrs. Gaynor Joyce[60]) are also available from R.A.E., Farnborough.

5. *Wave Properties.*

5.1. *Properties which depend on Heat Release and the Normal Component of Upstream Mach Number.*

From equation (10),

$$\frac{u_2}{u_1} = \left(\frac{\rho_2}{\rho_1}\right)^{-1} = 1 - F\frac{M_{N1}^2 - 1}{(\gamma+1)\, M_{N1}^2}. \tag{12}$$

It follows from equations (2), (5) and (12) that

$$\frac{p_2}{p_1} = 1 + \frac{p_2 - p_1}{p_1} = 1 + \frac{\rho_1 u_1 (u_1 - u_2)}{p_1} = 1 + \gamma M_{N1}^2 \left(1 - \frac{u_2}{u_1}\right).$$

Therefore

$$\frac{p_2}{p_1} = 1 + \gamma F \frac{M_{N1}^2 - 1}{\gamma + 1}. \tag{13}$$

Also, since the mean molecular weight of the mixture is assumed not to change across the wave,

$$\frac{T_2}{T_1} = \frac{p_2}{p_1}\frac{\rho_1}{\rho_2} = \left(1 + \gamma F\frac{M_{N1}^2 - 1}{\gamma+1}\right)\left(1 - F\frac{M_{N1}^2 - 1}{(\gamma+1)\, M_{N1}^2}\right) \tag{14}$$

and

$$\frac{M_{N2}}{M_{N1}} = \frac{u_2}{u_1}\frac{a_1}{a_2} = \sqrt{\frac{p_1\, \rho_1}{p_2\, \rho_2}} = \sqrt{\left(1 - F\frac{M_{N1}^2 - 1}{(\gamma+1)\, M_{N1}^2}\right)\Big/\left(1 + \gamma F\frac{M_{N1}^2 - 1}{\gamma+1}\right)}. \tag{15}$$

The Rankine-Hugoniot equation may be derived from equations (12) and (13) as

$$\frac{\rho_2}{\rho_1} = \left[\left(\frac{\gamma F}{\gamma+1} - 1\right) + \frac{p_2}{p_1}\right] \Big/ \left[(F-1) + \left(1 - \frac{F}{\gamma+1}\right)\frac{p_2}{p_1}\right], \tag{16}$$

or for Chapman-Jouguet waves as

$$\frac{\rho_2}{\rho_1} = 1 + \frac{1}{\gamma}\left(1 - \frac{p_1}{p_2}\right); \tag{17}$$

for shock waves ($F = 2$), equation (16) simplifies to the standard form,

$$\frac{\rho_2}{\rho_1} = \left(\frac{\gamma-1}{\gamma+1} + \frac{p_2}{p_1}\right) \Big/ \left(1 + \frac{\gamma-1}{\gamma+1}\frac{p_2}{p_1}\right). \tag{18}$$

All the above expressions are independent of M_1, the free-stream Mach number. It can also be shown that one other important parameter, namely the entropy rise across the wave is independent of M_1, *viz*:

$$ds = \frac{de}{T} + \frac{p}{T} d\left(\frac{1}{\rho}\right) = C_V \frac{dT}{T} + R\rho\, d\left(\frac{1}{\rho}\right) = \frac{R}{\gamma-1}\frac{dT}{T} + R\rho\, d\left(\frac{1}{\rho}\right);$$

so, for constant R and γ,

$$\frac{\Delta s}{R} = \frac{1}{\gamma-1}\int_1^2 \frac{dT}{T} + \int_1^2 \rho\, d\left(\frac{1}{\rho}\right) \tag{19}$$

i.e.

$$\frac{\Delta s}{R} = \frac{1}{\gamma-1}\log_e\left(\frac{T_2}{T_1}\right) + \log_e\left(\frac{\rho_2}{\rho_1}\right) \tag{20}$$

or

$$e^{-\Delta s/R} = \left(\frac{\rho_2}{\rho_1}\right)^{\frac{\gamma}{\gamma-1}} \Big/ \left(\frac{p_2}{p_1}\right)^{\frac{1}{\gamma-1}} = f(F, \gamma, M_{N1})$$

$$= \left[\frac{\gamma+1}{\gamma+1+\gamma F(M_{N1}^2 - 1)}\right]^{\frac{1}{\gamma-1}} \left[\frac{(\gamma+1)M_{N1}^2}{F + (\gamma+1-F)M_{N1}^2}\right]^{\frac{\gamma}{\gamma-1}}. \tag{21}$$

Alternatively, equation (20) may be written

$$\frac{\Delta s}{R} = \log_e\left(\frac{T_2}{T_1}\right)^{\frac{1}{\gamma-1}} + \log_e\left[\frac{R\,T_2}{R\,T_1}\frac{p_{T1}}{p_{T2}}\left(\frac{2+(\gamma-1)M_2^2}{2+(\gamma-1)M_1^2}\right)^{\frac{\gamma}{\gamma-1}}\right]$$

$$= \log_e\left[\frac{p_{T1}}{p_{T2}}\left(\frac{T_{T2}}{T_{T1}}\right)^{\frac{\gamma}{\gamma-1}}\right]$$

or

$$e^{-\Delta s/R} = \frac{p_{T2}}{p_{T1}} \Bigg/ \left(\frac{T_{T2}}{T_{T1}}\right)^{\frac{\gamma}{\gamma-1}}. \tag{22}$$

Note that across a shock wave, stagnation temperature does not change (because $T_{T2}/T_{T1} = 1 + (q/C_p T_{T1})$), so that for a given value of γ, both the entropy rise and the stagnation pressure ratio are independent of M_1; however, across a detonation wave, the stagnation temperature rises due to the release of heat ($q \neq 0$), so that the stagnation pressure ratio across a detonation is partially dependent on the rise in stagnation temperature and becomes a function of both normal and streamwise components of upstream Mach number. Study of stagnation pressure is therefore reserved for Section 5.2 (and Appendix C).

It has so far been shown that u_2/u_1, ρ_2/ρ_1, p_2/p_1, T_2/T_1, M_{N2}/M_{N1} and $\Delta s/R$ are functions $f(F, \gamma, M_{N1})$. If, as an alternative to F, a parameter for quoting heat release is defined as

$$A \equiv F\frac{M_{N1}^2-1}{\gamma+1},$$

then the above functions may be summarised as follows:

$$\frac{u_2}{u_1} = \left(\frac{\rho_1}{\rho_2}\right)^{-1} = 1 - F\frac{M_{N1}^2-1}{(\gamma+1)M_{N1}^2} = 1 - \frac{A}{M_{N1}^2} \tag{23}$$

$$\frac{p_2}{p_1} = 1+\gamma F\frac{M_{N1}^2-1}{\gamma+1} = 1+\gamma A \tag{24}$$

$$\frac{T_2}{T_1} = \left(1+\gamma F\frac{M_{N1}^2-1}{\gamma+1}\right)\left(1-F\frac{M_{N1}^2-1}{(\gamma+1)M_{N1}^2}\right) = (1+\gamma A)\left(1-\frac{A}{M_{N1}^2}\right) \tag{25}$$

$$\frac{M_{N2}}{M_{N1}} = \sqrt{\left(1-F\frac{M_{N1}^2-1}{(\gamma+1)M_{N1}^2}\right)\Bigg/\left(1+\gamma F\frac{M_{N1}^2-1}{\gamma+1}\right)} = \sqrt{\left(1-\frac{A}{M_{N1}^2}\right)\Big/(1+\gamma A)} \tag{26}$$

$$e^{-\Delta s/R} = \left[\frac{\gamma+1}{\gamma+1+\gamma F(M_{N1}^2-1)}\right]^{\frac{1}{\gamma-1}}\left[\frac{(\gamma+1)M_{N1}^2}{F+(\gamma+1-F)M_{N1}^2}\right]^{\frac{\gamma}{\gamma-1}}$$

$$= 1\Bigg/\left[(1+\gamma A)^{\frac{1}{\gamma-1}}\left(1-\frac{A}{M_{N1}^2}\right)^{\frac{\gamma}{\gamma-1}}\right]. \tag{27}$$

For a chosen value of γ, these relations (23) to (27) could be shown graphically as in Figs. 2 to 6, heat release being shown as F (or A) or as Damköhler's second parameter, $q/C_p T_1$; such charts would be valid for plane shocks or Chapman-Jouguet or strong detonations, which occur as normal or oblique waves in uniform supersonic streams of pure or pre-mixed gas.

Alternatively, these relations may be presented more compactly in the upper pair of the graphically inter-related charts of Fig. 7. In Fig. 7b as shown in Appendix A, lines of constant M_{N2}/M_{N1} and constant M_{N1} form families of straight lines, each family with its own focal point; lines of constant T_2/T_1 form a family of rectangular hyperbolae and lines of constant F are asymptotic to values of ρ_2/ρ_1 given by

$$\frac{\rho_1}{\rho_2} = 1 - \frac{F}{\gamma+1}. \tag{28} \quad (A.3)$$

Also as shown in Appendix A, the variables chosen in Fig. 7c allow it to show the variation of wave and deflection angles, and of the stream tube contraction ratio (A_2/A_1), which would occur with oblique shock or detonation waves. Finally as confirmed in Fig. 7c, a maximum deflection condition occurs for waves with which

$$\tan^2 \zeta = \rho_2/\rho_1 . \qquad (29) \quad (A.6)$$

Figs. 7 a to c have been constructed without any reference to M_1, the up-stream Mach number. This is introduced in Fig. 7d in which lines of constant M_{N1} ($= M_1 \sin \zeta$) are plotted on axes showing ζ and M_1. As explained in Appendix A, the condition for maximum deflection gives a single locus for each value of F in the range $1 \leqslant F \leqslant 2$; as $M_1 \to \infty$, each locus is asymptotic to a line which corresponds to the asymptote for the same value of F in Fig. 7b, and in Fig. 7c would intersect that asymptote on the maximum deflection line (e.g. for $F = 1$ and 2, intersections occur at P_1 and P_2 respectively).

For many purposes it is more convenient to express wave and deflection angles respectively as functions of M_{N1} and M_1, and of F, γ, M_{N1} and M_1—discussion of these and other properties is presented in Section 5.2.

5.2. *Properties which depend on Heat Release and both Normal and Streamwise Components of Up-stream Mach Number.*

It is shown in Appendix B that flow deflection δ is given by the expression,

$$\cot \delta = \left(\frac{M_1^2 (\gamma+1)}{F(M_{N1}^2 - 1)} - 1 \right) \Big/ \sqrt{\left(\frac{M_1}{M_{N1}}\right)^2 - 1} \; ; \qquad (30) \quad (B.2)$$

it is further shown that for waves of a given F-value, the condition for maximum deflection for a given value of M_{N1} is

$$\tan^2 \zeta = \rho_2/\rho_1 \qquad (31) \quad (A.6) \quad (B.3)$$

i.e.

$$\delta_{max} \Big]_{M_{N1}} = 2\zeta - (\pi/2) . \qquad (32) \quad (B.5)$$

For a given γ and F, all properties which are independent of M_1 may be plotted against δ (as in Fig. 8) in the form of a 'scroll' or three-dimensional carpet showing M_1 and ζ ($\equiv \sin^{-1}(M_{N1}/M_1)$); further since M_{N1} is an axis variable, the envelope to this carpet is given by equation (31). As an alternative to Fig. 8, ζ may be plotted against δ, as in Fig. 9. It is then seen that two δ_{max} conditions exist, one for constant M_{N1} as expressed by equation (31) and one for constant M_1. On axes of ζ and δ the locus for $\delta_{max}\Big]_{M_{N1}}$ is a straight line (*see* equation (32) (B.5)) and that for $\delta_{max}\Big]_{M_1}$ is known from Appendix B, that is,

$$\sin^2 \zeta = \left(\frac{M_{N1}}{M_1}\right)^2$$

$$= M_{N1}^2 (M_{N1}^2 + 1)(\gamma+1)/[2(\gamma+1)M_{N1}^4 - F(M_{N1}^2 - 1)^2]$$

$$= \left[(\gamma+1)M_1^2 - 2F \pm \sqrt{(\gamma+1)[(\gamma+1)M_1^4 + 8(\gamma+1-F)M_1^2 + 8F]} \right] \Big/ 2[2(\gamma+1) - F]M_1^2 . \qquad (33) \quad (B.8)$$

Note that as M_1 and M_{N1} increase to infinity, the difference between values of ζ for a given deflection becomes infinitesimal. The line corresponding to $M_1 = \infty$ is found from equation (30) (B.2) thus

$$\cot \delta = \left(\frac{M_1^2(\gamma+1)}{F(M_{N1}^2-1)} - 1 \right) \Big/ \sqrt{\left(\frac{M_1}{M_{N1}}\right)^2 - 1}$$

$$= \left(\frac{\gamma+1}{F\left(\sin^2 \zeta - \dfrac{1}{M_1^2}\right)} - 1 \right) \Big/ \sqrt{\operatorname{cosec}^2 \zeta - 1} \; ;$$

hence if $M_1 = \infty$,

$$\cot \delta \Big]_{M_1=\infty} = \tan \zeta \left(\frac{\gamma+1}{F \sin^2 \zeta} - 1 \right).$$

As further shown in Appendix B, the absolute maximum value of δ is given by the expression,

$$\cot \delta_{\substack{\text{abs}\\ \text{max}}} = \frac{2(\gamma+1)}{F} \sqrt{1 - \frac{F}{\gamma+1}}, \qquad (34) \quad (B.10)$$

for which

$$\zeta = \tfrac{1}{2} \delta_{\substack{\text{abs}\\ \text{max}}} + (\pi/4) \qquad (35) \quad (B.5)$$

and

$$\sin \zeta \Big]_{\delta_{\substack{\text{abs}\\ \text{max}}}} = \sqrt{1 \Big/ \left(2 - \frac{F}{\gamma+1}\right)}. \qquad (36) \quad (B.9)$$

Values of δ and ζ at this absolute maximum condition are given, for $\gamma = 1{\cdot}4$ and various values of F, in Table 4; it is seen that shock waves give the greatest deflection of all (45·5847°) and Chapman-Jouguet waves the least (15·2575°).

Also shown in Fig. 9 are a few lines of constant discharge Mach number, M_2. From Fig. 1,

$$M_2 = M_{N2} \operatorname{cosec} (\zeta - \delta) \; ;$$

thus for the particular case of Chapman-Jouguet waves ($F = 1 = M_{N2}$),

$$\zeta = \delta + \operatorname{cosec}^{-1} M_2$$

and for a given value of M_2, $d\zeta/d\delta = 1 =$ const. Thus for Chapman-Jouguet waves, lines of constant M_2, plotted on axes of ζ and δ, are parallel and straight. It is for the particular case of Chapman-Jouguet waves that lines of constant M_2 are drawn in Fig. 9.

A more general expression for discharge Mach number can be derived from that for the velocity ratio, which from Fig. 1 is seen to be

$$\frac{V_2}{V_1} = \frac{\cos \zeta}{\cos (\zeta - \delta)} = \sqrt{\frac{1+\tan^2 (\zeta-\delta)}{1+\tan^2 \zeta}} = \sqrt{\frac{1+(\rho_1/\rho_2)^2 \tan^2 \zeta}{1+\tan^2 \zeta}},$$

i.e.

$$\frac{V_2}{V_1} = \sqrt{1 - \frac{F(M_{N1}^2-1)[2(\gamma+1)M_{N1}^2 - F(M_{N1}^2-1)]}{(\gamma+1)^2 M_{N1}^2 M_1^2}}. \tag{37}$$

In Fig. 10, velocity ratio is plotted against flow deflection as a carpet of M_{N1} and ζ; some lines of constant M_1 and M_2 are also shown. The line corresponding to $M_1 = \infty$ is found from equation (37) thus:

$$\frac{V_2}{V_1} = \sqrt{1 - \frac{F\left(\sin^2\zeta - \frac{1}{M_1^2}\right)\left[2(\gamma+1)\sin^2\zeta - F\left(\sin^2\zeta - \frac{1}{M_1^2}\right)\right]}{(\gamma+1)^2 \sin^2\zeta}};$$

hence if $M_1 = \infty$,

$$\left.\frac{V_2}{V_1}\right]_{M_1=\infty} = \sqrt{1 - \frac{F}{\gamma+1}\left(2 - \frac{F}{\gamma+1}\right)\sin^2\zeta}.$$

The expression for stream Mach number ratio is then

$$\frac{M_2}{M_1} = \frac{V_2}{V_1}\frac{a_1}{a_2} = \sqrt{\frac{(\gamma+1)^2 M_{N1}^2 - F(M_{N1}^2-1)[2(\gamma+1)M_{N1}^2 - F(M_{N1}^2-1)]/M_1^2}{(\gamma+1+\gamma F(M_{N1}^2-1))(F+(\gamma+1-F)M_{N1}^2)}} \tag{38}$$

In Fig. 11, discharge Mach number is plotted against flow deflection as a carpet of M_{N1}, ζ and M_1; this is considered more useful than a plot of Mach number ratio (M_2/M_1), but such a plot is possible and a sketch is shown inset.

In Appendix C, it is shown that the stagnation temperature ratio across a wave is given by the expression

$$\frac{T_{T2}}{T_{T1}} = 1 + \frac{F(2-F)(M_{N1}^2-1)^2}{(\gamma+1)M_{N1}^2(2+(\gamma-1)M_1^2)} \qquad (39) \quad (C.1)$$

In Fig. 12, stagnation temperature ratio is plotted against flow deflection, as a three-dimensional carpet showing M_{N1}, ζ, M_2 and some lines of constant M_1. This carpet has an envelope given by the condition

$$M_1^2 = \frac{(M_{N1}^2+1)(M_{N1}^2(2(\gamma+1)-F)+F)}{F(\gamma-1)(M_{N1}^2-1)+(\gamma+1)(1+(2-\gamma)M_{N1}^2)}. \qquad (40) \quad (C.2)$$

The remainder of the carpet boundary corresponds to $M_1 = \infty$, i.e. from equation (39), to the condition

$$\frac{T_{T2}}{T_{T1}} = 1 + \frac{F(2-F)\sin^2\zeta}{(\gamma+1)(\gamma-1)};$$

from this equation, the overall maximum value of T_{T2}/T_{T1} is seen to result with a normal Chapman-Jouguet wave ($\zeta = 90°$, $F = 1$), for which the stagnation temperature ratio reaches the value $\gamma^2/(\gamma^2-1)$ i.e. $2{\cdot}041\dot{6}$ if $\gamma = 1{\cdot}4$.

For the more oblique wave solution at a given value of F and of flow deflection, values of T_{T2}/T_{T1} lie within the narrow 'crescent' formed between the envelope and one end of the line for $M_1 = \infty$; they are thus only weakly dependent on the particular combination of values chosen for M_{N1} and M_1.

The equation for stagnation pressure ratio is

$$\frac{p_{T2}}{p_{T1}} = \left(\frac{T_{T2}}{T_{T1}}\right)^{\frac{\gamma}{\gamma-1}} e^{-\Delta s/R}$$

$$= \left[\frac{\gamma+1}{\gamma+1+\gamma F(M_{N1}^2-1)}\right]^{\frac{1}{\gamma-1}} \left[\frac{(\gamma+1)M_{N1}^2}{F+(\gamma+1-F)M_{N1}^2} + \frac{F(2-F)(M_{N1}^2-1)^2}{(F+(\gamma+1-F)M_{N1}^2)(2+(\gamma-1)M_1^2)}\right]^{\frac{\gamma}{\gamma-1}}. \qquad (41) \quad (C.3)$$

In Fig. 13, the variation of stagnation pressure ratio with flow deflection is shown as a three-dimensional carpet of constant M_{N1}, ζ, M_1 and M_2; for Chapman-Jouguet waves the envelope condition for such a carpet is shown in Appendix C to be given by a cubic equation in p,

$$p^3 + C_1 p^2 + C_2 p + C_3 = 0,$$

in which C_1, C_2 and C_3 are functions of γ and M_{N1}, and

$$p+2 = 2+(\gamma-1)M_1^2 = (M_{N1}^2-1)^2 (\gamma+1)^{\frac{1}{\gamma}} \Bigg/ \left[\left(\frac{p_{T2}}{p_{T1}}\right)^{\frac{\gamma-1}{\gamma}} (1+\gamma M_{N1}^2)^{\frac{\gamma+1}{\gamma}} - (\gamma+1)^{\frac{\gamma+1}{\gamma}} M_{N1}^2\right]$$

$$= f_1(\gamma, M_1) = f_2(\gamma, M_{N1}, p_{T2}/p_{T1}) \qquad (42) \quad (C.4)$$

Values of p_{T2}/p_{T1}, δ, M_1 etc which correspond to this envelope condition (for Chapman-Jouguet waves and $\gamma = 1{\cdot}4 = $ const.) are given in Table 5.

6. *Final Comments.*

For quoting the heat release across normal or oblique detonation waves, a parameter F has been introduced, F being a function of the ratio of specific heats, the upstream static enthalpy and the component of upstream Mach number normal to the wave; for Chapman-Jouguet waves $F = 1$, for any strong detonation $1 < F < 2$, and for shock waves $F = 2$.

For detonation waves in non-dissociating air properties are shown to be functions $f(F, \gamma, M_{N1})$ or $f(F, \gamma_1, M_{N1}, M_1)$. The first group includes the ratios of static pressure, density and temperature, normal components of Mach number and velocity, and also the entropy rise; the second group includes the ratios of stream Mach number and of stream velocity, stagnation temperature and pressure, and the flow deflection angle.

It is noted that for shock waves (i.e. $F = 2$), the stagnation pressure ratio can be expressed as a function of γ and M_{N1}, but that for a detonation wave of specified type (i.e. having a specified F-value), the stagnation pressure ratio is a function of γ, M_{N1} and also M_1.

Formulae for maximising flow deflection at various conditions (constant M_{N1} or M_1, p_{T2}/p_{T1} or T_{T2}/T_{T1}) have been derived; these may assist in minimising structural problems (such as flexing or heating) of bodies upon which detonations of chosen type (F) and of specified heat release (F, γ, M_{N1}) are to be stabilised.

The analysis is performed for plane waves throughout. However, it may be combined with existing R.A.E. computer programmes (or those being developed) and so may allow computation of two-dimensional or axisymmetric flow fields formed between a body and a detonation wave.

LIST OF SYMBOLS

a	Velocity of sound
A	Defined as $A \equiv F \dfrac{M_N^2 - 1}{\gamma + 1}$; or with suffix refers to cross-sectional area of streamtube
c_p	Specific heat at constant pressure
c_q	Coefficient of heat release (*see* equation (11) and Ref. 52)
c_v	Specific heat at constant volume
e	Specific internal energy (also used as the base for natural logarithms)
F	Heat release parameter (*see* equation (10))
m	Molecular weight
M	Mach number
M_N	Component of Mach number (M) normal to wave
p	Static pressure (also used as defined in equation (42) (C.4))
p_T	Stagnation pressure
q	Heat released per unit mass
R	Gas constant
R	Universal gas constant
Δs	Change in specific entropy
T	Static temperature
T_T	Stagnation temperature
u	Component of stream velocity (V) normal to wave
v	Component of stream velocity (V) parallel to wave
V	Stream velocity
γ	Ratio of specific heats (i.e. c_p/c_v)
δ	Angle of flow deflection through wave
ζ	Angle of wave ($\equiv \sin^{-1} M_{N1}/M_1$, i.e. $\zeta = 90°$ for normal wave)
θ	Molecular vibrational-energy constant (*see* Ref. 59 equation (180))
ρ	Static density

Superscript

$*$	Refers to critical condition

Subscript

∞	Refers to free-stream conditions
1	Refers to region 1 in Fig. 1 (i.e. region upstream of wave)
2	Refers to region 2 in Fig. 1 (i.e. region downstream of wave)

REFERENCES

No.	*Author(s)*	*Title, etc.*
1	M. Berthelot	Sur la vitesse de propagation des phénomenes explosifs dans les gaz. *C.R. Acad. Sci.*, Paris. *93*, 18–22, 4 July 1881.
2	E. Mallard and H. Le Chatelier	Sur les vitesses de propagation de l'inflammation dans les mélanges gazeux explosifs. *C.R. Acad. Sci.*, Paris. *93*, 145–148, 18 July 1881.
3	D. L. Chapman	On the rate of explosion in gases. *Phil. Mag. 47*, 5th series, 284, 90–104, January 1899.
4	E. Jouguet	Sur la propagation des reactions chimiques dans les gaz. *J. Math. Pures et Appliqués, 6*, Serie 1, 347–425, 1905, 5–86, 1906.
5	Y. B. Zeldovich and O. I. Leypunskiy	Acta physiochim. URSS. 18, 167 (1943).
6	Y. B. Zeldovich and I. Y. Shlyapintokh	Bosplameneniye Vzryvchatykh Gasovykh Smesey v Udarnykh Volnakh. Doklady Akademii Nauk. SSSR, *65*, 6, 871–874, 1949. Available as 'Ignition of explosive gaseous mixtures in shock waves' from the Office of Technical Services U.S. Dept. of Commerce, Washington, D.C. OTS: 60–41, 533, 1960.
7	National Bureau of Standards	A technique for studying supersonic combustion in the vicinity of a hypersonic missile. *Nat. Bur. of Std. and Tech. News Bull., 44*, No. 11, 1960.
8	F. W. Ruegg and W. W. Dorsey	A missile technique for the study of detonation waves. *J. Res., Nat. Bur. of Stand., 66C*, No. 1, 1962.
9	M. P. Samozvantsev	O Stabilizatsii Detonatsionnykh Voln Pri Pomoshchi Plokhoobtekaemykh Tel, PMTF, No. 4, 126–129, 1964. Available as 'The stabilisation of detonation waves by means of bluff bodies', translated by J. W. Palmer, R.A.E. Library Trans. 1088, 1964.
10	H. Behrens, W. Struth and F. Wecken ..	Studies of hypervelocity firings into mixtures of hydrogen with air or oxygen. Paper presented to the Tenth (International) Symposium on Combustion, Cambridge, England, 1964.
11	H. Behrens and W. Struth ..	Verbrennungsvorgänge bei Hochgeschwindigkeitsschüssen mit Kegelgeschossen in Knallgas. Deutsch-Französisches Forschungsinstitut Saint-Louis. T41/64, 1964.
12	B. V. Voitsekhovsky and B. E. Kotov ..	Optical investigation of the front of spinning detonation wave. *Izv Sibirsk. Otd. Akad. Nauk.* SSSR4, 79, 1958.

No.	*Author(s)*	*Title, etc.*
13	B. V. Voitsekhovsky	'Stazionarnaia detonatsia.' *Doklady Akad. Nauk.* SSSR *129*, 6, 1254–1256, 1959.
14	B. V. Voitsekhovsky	'Spinovaia Statsionarnaia detonatsia'. *Zh. Prikl. Mekh. I. Techn.* Fiz. 3, 157–164, 1960.
15	B. V. Voitsekhovsky, ... V. V. Mitrofanov and M. E. Topchian	On the flow structure in a spinning detonation wave. *Zh. Prikl. Meckh. I. Techn.* Fiz. 3, 27–30, 1962.
16	J. A. Nicholls *et al*	The feasibility of a rotating detonation wave rocket motor. Quarterly Progress Report No. 2, 05179–2–P, University of Michigan. 1962. AD414551.
17	J. A. Nicholls *et al*	The feasibility of a rotating detonation wave rocket motor. Final Report R.P.L./TDR 64–113. 1964. Contract AF04(611)8503.
18	H. Hoffman	Rückstossantrieb aus intermittierender detonativer Verbrennung. Deutsche Forschungsanstalt für Segelflug E.V., Darmstadt-Flughafen. Volkenrode Translation by Ministry of Supply available as 'Reaction propulsion by intermittent detonative combustion' from Ministry of Aviation, England.
19	D. Bitondo and W. Bollay ..	Preliminary performance analysis of the pulse-detonation-jet engine system. Aerophysics Development Corp., Rept. ADC–102–1, 1952.
20	D. Bitondo, J. B. Kendrick .. and W. Bollay	Preliminary report on the application of the pulse-det-jet engine to helicopter rotor propulsion. Aerophysics Development Corp., Report ADC–102–3, 1952.
21	J. A. Nicholls, H. R. Wilkinson and J. B. Morrison	Intermittent detonation as a thrust-producing mechanism. Jet Propulsion, *27*, 5, 534–541. 1957.
22	J. A. Nicholls, E. K. Dabora .. and R. L. Gealer	Studies in connection with stabilised gaseous detonation waves. *Seventh Symposium (International) on combustion, London and Oxford*, 1958. Published by Butterworth's Scientific Publications, London, 1959.
23	R. A. Gross	Research on supersonic combustion. *ARS Journal 29*, 1, 63–64, 1959.
24	J. A. Nicholls	Stabilised gaseous detonation waves. *ARS Journal 29*, 8, 607, 1959.
25	J. A. Nicholls and E. K. Dabora	Recent results on standing detonation waves. University of Michigan. May 1960. AFOSR TN 60–441. ASTIA AD 238–393. P 92725.

No.	*Author(s)*	*Title, etc.*
26	R. A. Gross and W. Chinitz ..	A study of supersonic combustion. *J. Aero/Space Sci.*, July 1960 *27*, 7, 517–524, 1960.
27	A. A. Kovitz	Some comments on standing detonation waves in a combustion tunnel. *J. Aero/Space Sci. 28*, 1, 75–76, 1961.
28	J. A. Nicholls	Stabilisation of gaseous detonation waves with emphasis on the ignition delay zone. Ph. D. Thesis, University of Michigan, 1960.
29	R. A. Gross and J. A. Nicholls ..	Stationary detonation waves. 4th AGARD Combustion and Propulsion Colloquium on high Mach number air-breathing engines. Milan, April 1960, pp. 169–177.
30	R. P. Rhodes, P. M. Rubins and D. E. Chriss	The effect of heat release on the flow parameters in shock induced combustion. AEDC–TDR–62–78, 1962. See also SAE preprint 595P 1962.
31	P. M. Rubins and R. P. Rhodes	Shock induced combustion with oblique shocks—comparison of experiment and kinetic calculations. AEDC–TDR–63–103, 1963. Also AIAA preprint No. 63–117. Also AIAA Jl, *1*, 12, 2778–2784, 1963.
32	P. M. Rubins and T. H. M. Cunningham	Shock induced combustion in a controlled area duct by means of oblique shocks. AIAA preprint No. 64–84, 1964.
33	F. Suttrop	Tests on shock-induced combustion for application in hypersonic engines. T.I.L. Translation TP.1507A, 1965.
34	R. A. Gross and A. K. Oppenheim	Recent advances in gaseous detonation. *ARS Journal*, *29*, No. 3, 173–179, 1959.
35	A. K. Oppenheim, N. Manson and H. Gg. Wagner	Recent progress in detonation research. *AIAA Journal*, *1*, No. 10, 2243–2252, 1963.
36	Library of Congress, Aero/ Space Technology Division ..	New combustion processes: surveys of Soviet-bloc scientific and technical literature (1958–January 1964). Library of Congress, Washington, D.C., ATD–P–64–49, NASA 64–27342, 1964.
37	R. Dunlap, R. L. Brehm and J. A. Nicholls ..	A preliminary study of the application of steady-state detonative combustion to a reaction engine. *Jet Propulsion*, *28*, 6, 451–456. 1958.

No.	*Author(s)*	*Title, etc.*
38	W. H. Sargent and R. A. Gross	Detonation wave hypersonic ramjet. *ARS Journal*, *30*, 6, 543–549, 1960.
39	E. Larisch	The ramjet with standing detonation wave. Paper presented at the meeting of the Romanian Academy, Timisoara, 1958.
40	M. Arens	The performance of a hypersonic ramjet using detonative combustion. SAE preprint 419A. Paper presented to the National Aeronautic and Space Engineering and Manufacturing Meeting, Los Angeles, California, 1961.
41	K. M. Foreman	Terrestrial hypersonic flight propulsion. AIAA preprint No. 63–110, 1963.
42	A. Mager	Supersonic airfoil performance with small heat addition. IAS preprint No. 768, 1958. Also *J. Aero/Space Sci.*, *26*, No. 2, 1959.
43	H. Lomax	Two-dimensional, supersonic, linearized flow with heat addition. NASA Memo. 1–10–59A. 1959. NASA TIL 6196.
44	R. W. Luidens and R. J. Flaherty	Analysis and evaluation of supersonic underwing heat addition. NASA Memo 3–17–59E, 1959. NASA TIL 6345.
45	W. W. Willmarth	The production of aerodynamic forces by heat addition on external surfaces of aircraft. The Rand Corp. RM–2078, December 1957.
46	B. S. Baldwin, Jr.	Application to fluid dynamics of the theory of reversible heat addition. NASA TN D–93. 1959.
47	A. K. Oppenheim and A. J. Laderman ..	Significance of detonation study to propulsion dynamics. Univ. of California, Berkeley, U.S.A. AD 421130, N 64–32873. 1964.
48	J. Rutkowski and J. A. Nicholls.	Considerations for the attainment of a standing detonation wave. Gas Dynamics Symposium of Aerothermochemistry, Northwestern University, 243–253, 1955.
49	R. Seistrunck, J. Fabri and E. Le Grives ..	Some properties of stationary detonation waves. Fourth Symposium on Combustion, Williams and Wilkins Co., Baltimore, 498–501, 1953.
50	W. Chinitz, L. C. Bohrer and K. M. Foreman ..	Properties of oblique detonation waves. Fairchild Engine Division, AFOSR TN 59–462 (ASTIA AD 215–267), 1959. P 105, 384.

No.	*Author(s)*	*Title, etc.*
51	D. G. Samaras	Gas dynamic treatment of exothermic and endothermic discontinuities. *Canadian Journal of Research, 26A*, No. 1, 1–21, 1948.
52	J. Weber	Some diagrams of the flow properties behind oblique detonation waves. R.A.E. unpublished.
53	S. S. Kvashnina and G. G. Chernyi	Ustanovivsheesia obtekanie Konusa potokom detoniruiuschchego gaza. PMM *23*, No. 1 182–186, 1959. Available as 'Steady state flow of detonating gas around a cone' translated and published for ASME by the Pergamon Institute.
54	H. W. Woolard	Analytical approximations for stationary conical detonations and deflagrations in supersonic flow. Applied Physics Lab., John Hopkins University, TG–446, 1963.
55	T. C. Adamson, Jr., and R. B. Morrison ..	On the classification of normal detonation waves. *Jet Propulsion. 25*, No. 8, pp. 400 and 403, 1955.
56	R. S. Bartlett	Tables of supersonic symmetrical flow around right circular cones with and without the addition of heat at the wave. A.R.C. R. & M. 3521, 1966.
57	F. Walkden and J. M. Howie ..	A new method for calculating the supersonic flow past a body. R.A.E. Tech. Note. No. Maths 89, 1962. A.R.C. 24 350.
58	F. Walkden and J. E. Sellars ..	A 'pseudo-viscous' method for the calculation of two-dimensional supersonic flow fields. R.A.E. Tech. Rpt. No. 65009, 1965. A.R.C. 26 745.
59	Ames Aeronautical Laboratory, Moffett Field	Equations, tables, and charts for compressible flow. NACA RM 1135, 1953.
60	Gaynor Joyce and L. H. Townend	Flow tables for oblique and normal detonation waves. R.A.E. unpublished.

APPENDIX A

Features of Fig. 7.

For waves across which γ does not vary, it has been shown in equations (23) to (26) of Section 5.1 that

$$\frac{u_2}{u_1} = \left(\frac{\rho_2}{\rho_1}\right)^{-1} = 1 - \frac{A}{M_{N1}^2}, \quad \left(A \equiv F\frac{M_{N1}^2 - 1}{\gamma + 1}\right) \qquad \text{(A.1)}$$

$$\frac{p_2}{p_1} = 1 + \gamma A \qquad \text{(A.2)}$$

$$\frac{T_2}{T_1} = (1+\gamma A)\left(1 - \frac{A}{M_{N1}^2}\right)$$

$$\frac{M_{N2}}{M_{N1}} = \sqrt{\left(1 - \frac{A}{M_{N1}^2}\right)\Big/(1+\gamma A)}$$

γ constant

It follows that, if plotted on axes of p_2/p_1 and ρ_1/ρ_2 $\left(\text{i.e. of } (1+\gamma A) \text{ and } \left(1 - \frac{A}{M_{N1}^2}\right)\right)$, lines of constant T_2/T_1 will be rectangular hyperbolae having the axes as asymptotes. Further

$$\frac{\rho_1}{\rho_2} = \left(\frac{M_{N2}}{M_{N1}}\right)^2 \frac{p_2}{p_1};$$

hence lines of constant M_{N2}/M_{N1} form straight lines through the point ($\rho_1/\rho_2 = p_2/p_1 = 0$). Also from (A.1) and (A.2)

$$\frac{p_2}{p_1} = 1 + \gamma A = (1 + \gamma M_{N1}^2) - \gamma M_{N1}^2 \left(\frac{\rho_1}{\rho_2}\right)\left(= 1 \text{ if } \frac{\rho_1}{\rho_2} = 1\right);$$

hence, lines of constant M_{N1}, plotted on axes of p_2/p_1 and ρ_1/ρ_2 form a family of straight lines through the point ($p_2/p_1 = 1, \rho_1/\rho_2 = 1$). Lines of constant T_2/T_1, M_{N2}/M_{N1} and M_{N1} are shown with others on axes of p_2/p_1 and ρ_1/ρ_2 in Fig. 7b. Also in this Figure, asymptotes may be drawn for any line along which F is constant, since the asymptote condition is

$$\underset{M_{N1}\to\infty}{Lt} \frac{\rho_1}{\rho_2} = \underset{M_{N1}\to\infty}{Lt} \left(1 - F\frac{M_{N1}^2 - 1}{(\gamma+1) M_{N1}^2}\right) = 1 - \frac{F}{\gamma+1}. \qquad \text{(A.3)}$$

So for shock waves, the asymptotic value of ρ_1/ρ_2 is

$$\frac{\rho_1}{\rho_2} = \frac{\gamma - 1}{\gamma + 1}\,(= 0{\cdot}1666 \quad \text{for} \quad \gamma = 1{\cdot}4),$$

and for Chapman-Jouguet detonations, the asymptotic value is

$$\frac{\rho_1}{\rho_2} = \frac{\gamma}{\gamma + 1}\,(= 0{\cdot}5833\dot{3} \quad \text{for} \quad \gamma = 1{\cdot}4)$$

Also from Fig. 1a,

$$\tan(\zeta-\delta) = \frac{u_2}{v_2} = \frac{u_2}{v_1} = \frac{u_1}{v_1}\frac{u_2}{u_1} = \frac{\rho_1}{\rho_2}\tan\zeta$$

and

$$\frac{A_2}{A_1} = \frac{\sin(\zeta-\delta)}{\sin\zeta} = \cos\delta - \frac{\sin\delta}{\tan\zeta};$$

thus

$$\frac{\rho_1}{\rho_2} = \frac{A_2}{A_1}\tan\delta \Big/ \left(\sec\delta - \frac{A_2}{A_1}\right) \tag{A.4}$$

and

$$\cot\zeta = \cot\delta - \frac{A_2}{A_1}\operatorname{cosec}\delta. \tag{A.5}$$

It is seen from equations (A.4) and (A.5) that a carpet of A_2/A_1 and δ may be plotted on axes of ρ_1/ρ_2 and ζ; this is shown in Fig. 7c, which like Figs. 7 a and b is valid for any normal or oblique, shock or detonation wave in any uniform flow having $M_1 > 1$. A final feature of Fig. 7c is that from (A.4) and (A.5)

$$\cot\delta = \tan\zeta\left(\frac{\operatorname{cosec}^2\zeta}{1-(\rho_1/\rho_2)} - 1\right),$$

so that maximum flow deflection, for given values of γ, F and M_{N1} (i.e. of ρ_1/ρ_2) occurs when

$$\frac{\partial}{\partial\zeta}(\cot\delta) = \frac{\partial}{\partial\zeta}\left[\tan\zeta\left(\frac{\operatorname{cosec}^2\zeta}{1-(\rho_1/\rho_2)} - 1\right)\right] = 0$$

i.e. when

$$\tan^2\zeta = \rho_2/\rho_1; \tag{A.6}$$

since $\sin\zeta = M_{N1}/M_1$, this condition may be re-written from equation (A.1) as

$$M_1^2 = M_{N1}^2\left(2-\frac{F}{\gamma+1}\right) + \frac{F}{\gamma+1} = 2M_{N1}^2 \quad \begin{cases} = \dfrac{2(1+\gamma M_{N1}^2)}{(\gamma+1)} \text{ for shock waves} \\[2ex] \dfrac{1+(2\gamma+1)M_{N1}^2}{\gamma+1} \text{ for Chapman-Jouguet waves} \end{cases} \tag{A.7}$$

So for a given type of wave (i.e. a given F), a chosen value of M_{N1} yields a given value of M_1 and loci describing waves for which $\tan^2\zeta = \rho_2/\rho_1$ may be constructed on Fig. 7d. For a given type of wave, it is seen that ζ is nearly independent of M_1; a much fuller investigation of δ is presented in Appendix B and Section 5.2.

APPENDIX B

Flow Deflection through Oblique Detonation Waves.

In Fig. 1a:

$$u_1 = V_1 \sin \zeta , \quad u_2 = V_2 \sin (\zeta - \delta)$$

$$v_1 = V_1 \cos \zeta = v_2 = V_2 \cos (\zeta - \delta) .$$

Therefore

$$\tan (\zeta - \delta) = \frac{u_2}{v_2} = \frac{u_2}{v_1} = \frac{u_1}{v_1} \frac{u_2}{u_1} = \frac{\rho_1}{\rho_2} \tan \zeta .$$

Therefore

$$\cot \delta = \tan \zeta \left(\frac{\operatorname{cosec}^2 \zeta}{1 - (\rho_1/\rho_2)} - 1 \right) \tag{B.1}$$

But

$$\left. \begin{aligned} \tan^2 \zeta &= \sin^2 \zeta / (1 - \sin^2 \zeta) \\ \operatorname{cosec}^2 \zeta &= 1/\sin^2 \zeta \end{aligned} \right\} \sin^2 \zeta = \left(\frac{M_{N1}}{M_1} \right)^2 .$$

and

Also

$$\frac{\rho_1}{\rho_2} = 1 - F \frac{M_{N1}^2 - 1}{(\gamma + 1) M_{N1}^2}$$

(*see* equation (12)).

Thus

$$\cot \delta = \left(\frac{M_1^2(\gamma+1)}{F\,(M_{N1}^2 - 1)} - 1 \right) \Bigg/ \sqrt{\left(\frac{M_1}{M_{N1}} \right)^2 - 1} . \tag{B.2}$$

It has already been shown that for given values of γ, F and M_{N1}, maximum flow deflection occurs when

$$\tan^2 \zeta = \rho_2 / \rho_1 \qquad \text{(A.6)} \quad \text{(B.3)}$$

i.e.

$$M_1^2 = M_{N1}^2 \left(2 - \frac{F}{\gamma + 1} \right) + \frac{F}{\gamma + 1} = 2M_{N1}^2 - 1 \begin{cases} = \dfrac{2(1 + \gamma M_{N1}^2)}{\gamma + 1} & \text{for shock waves} \\[2ex] = \dfrac{1 + (2\gamma + 1) M_{N1}^2}{\gamma + 1} & \text{for Chapman-Jouguet waves} \end{cases} \qquad \text{(A.7)} \quad \text{(B.4)}$$

It can also be shown from equations (B.1) and (B.3), that

$$\cot \delta_{max}\Big]_{M_{N1}} = \frac{2\cot\zeta}{1-\cot^2\zeta} = \frac{2\tan\zeta}{\tan^2\zeta-1} = -\cot 2\zeta$$

i.e.

$$\tan 2\zeta = -\frac{1}{\tan\left(\delta_{max}\Big]_{M_{N1}}+\frac{\pi}{2}-\frac{\pi}{2}\right)} = -\frac{\tan\left(\delta_{max}\Big]_{M_{N1}}+\frac{\pi}{2}\right)+\cot\frac{\pi}{2}}{\tan\left(\delta_{max}\Big]_{M_{N1}}+\frac{\pi}{2}\right)\cot\frac{\pi}{2}-1}$$

Therefore

$$\zeta = \tfrac{1}{2}\,\delta_{max}\Big]_{M_{N1}}+\frac{\pi}{4},\ \frac{d}{d\zeta}\left(\delta_{max}\Big]_{M_{N1}}\right) = 2 \text{ (both expressions independent of } F\text{)} \qquad \text{(B.5)}$$

Further, from equations (B.2) and (B.4),

$$\cot \delta_{max}\Big]_{M_{N1}} = 2\frac{M_{N1}^2}{A}\sqrt{1-\frac{A}{M_{N1}^2}} = \sqrt{\left(\frac{M_1^2}{A}\right)^2-1} \qquad \text{(B.6)}$$

or

$$\cot \delta_{max}\Big]_{M_{N1}} = \frac{2M_{N1}^2(\gamma+1)}{F(M_{N1}^2-1)}\sqrt{1-F\frac{M_{N1}^2-1}{(\gamma+1)M_{N1}^2}} = \sqrt{\frac{M_1^2(\gamma+1)\left(2-\frac{F}{\gamma+1}\right)}{F(M_1^2-2)-\left(2-\frac{F}{\gamma+1}\right)}} \qquad \text{(B.7)}$$

Further formulae may be derived for those conditions at which δ is maximised for given values of γ and stream Mach number M_1, that is for the condition

$$\frac{\partial}{\partial M_{N1}}(\cot\delta) = 0\ ;$$

thus, differentiation of equation (B.2) yields the expression

$$\sin\zeta = \left(\frac{M_{N1}}{M_1}\right)_{\delta_{max}\big]_{M_1}} = \sqrt{\frac{M_{N1}^2(M_{N1}^2+1)(\gamma+1)}{2(\gamma+1)M_{N1}^4-F(M_{N1}^2-1)^2}}$$

$$= \sqrt{\frac{(\gamma+1)M_1^2-2F\pm\sqrt{(\gamma+1)\left[(\gamma+1)M_1^4+8(\gamma+1-F)M_1^2+8F\right]}}{2(2(\gamma+1)-F)M_1^2}} \qquad \text{(B.8)}$$

and from these expressions and equation (B.2), $\delta_{max}\Big]_{M_1}$ may be calculated (for values of M_{N1}, M_1, ζ

and $\delta_{max}\Big]_{M_1}$, *see* Table 3).

The wave angle for absolute maximum flow deflection is given by the limiting values of the expressions (B.8), that is

$$\sin\zeta\Big]_{\delta_{\substack{abs\\max}}} = \underset{M_{N1}\to\infty}{Lt}\frac{1}{\sqrt{1+(\rho_1/\rho_2)}} = \underset{M_{N1}\to\infty}{Lt}\sqrt{\frac{M_{N1}^2(M_{N1}^2+1)(\gamma+1)}{2(\gamma+1)M_{N1}^4-F(M_{N1}^2-1)^2}}$$

or

$$\sin\zeta\Big]_{\delta_{\substack{abs\\max}}} = \underset{M_1\to\infty}{Lt}\sqrt{\frac{(\gamma+1)M_1^2-2F\pm\sqrt{(\gamma+1)\,[(\gamma+1)M_1^4+8\,(\gamma+1-F)M_1^2+8F]}}{2(2(\gamma+1)-F)M_1^2}}$$

Therefore

$$\sin\zeta\Big]_{\delta_{\substack{abs\\max}}} = \sqrt{\frac{1}{2-\dfrac{F}{\gamma+1}}}\begin{cases} = \sqrt{\dfrac{\gamma+1}{2\gamma}} & \text{for shock waves} \\ = \sqrt{\dfrac{\gamma+1}{2\gamma+1}} & \text{for Chapman-Jouguet detonations}\end{cases} \tag{B.9}$$

Also the absolute maximum flow deflection angle is given by the limiting values of the expressions (B.7) as

$$\cot\delta_{\substack{abs\\max}} = \underset{M_{N1}\to\infty}{Lt}\frac{2M_{N1}^2(\gamma+1)}{F(M_{N1}^2-1)}\sqrt{1-F\frac{M_{N1}^2-1}{(\gamma+1)M_{N1}^2}}$$

$$= \underset{M_1\to\infty}{Lt}\sqrt{\left[\frac{M_1^2(\gamma+1)\left(2-\dfrac{F}{\gamma+1}\right)}{F(M_1^2-2)-\left(2-\dfrac{F}{\gamma+1}\right)}\right]^2-1}$$

$$= \frac{2(\gamma+1)}{F}\sqrt{1-\frac{F}{\gamma+1}}\begin{cases} = \sqrt{(\gamma+1)(\gamma-1)} & \text{for shock waves} \\ = 2\sqrt{\gamma(\gamma+1)} & \text{for Chapman-Jouguet detonations}\end{cases} \tag{B.10}$$

For $\gamma = 1{\cdot}4$ and $F = 1(0{\cdot}01)2$, values of $\delta_{\substack{abs\\max}}$ and $\zeta\Big]_{\delta_{\substack{abs\\max}}}$ are listed in Table 4.

$$= \left(\frac{\gamma+1}{\gamma+1+\gamma F(M_{N1}^2-1)} \right)^{\frac{1}{\gamma-1}} \left(\frac{(\gamma+1)M_{N1}^2}{F+(\gamma+1-F)M_{N1}^2} + \frac{F(2-F)(M_{N1}^2-1)^2}{(F+(\gamma+1-F)M_{N1}^2)(2+(\gamma-1)M_1^2)} \right)^{\frac{\gamma}{\gamma-1}} \quad \text{(C.3)}$$

If for a Chapman-Jouguet wave and constant γ (= 1·4), p_{T2}/p_{T1} is plotted against δ as in Fig. 13, the envelope of the (three-dimensional) carpet showing M_{N1} and M_1 represents the necessary relation between these two variables if flow deflection at a given value of p_{T2}/p_{T1} is to be maximised; from Fig. 13 it can be seen that this envelope condition is

$$\frac{\partial \delta}{\partial M_{N1}} \left(\text{or} \frac{\partial}{\partial (M_{N1}^2)} \cot \delta \right) = 0,$$

i.e.

$$\frac{\partial}{\partial (M_{N1}^2)} \left[\frac{(\gamma+1)p}{(\gamma-1)(M_{N1}^2-1)} - 1 \right] \Big/ \sqrt{\frac{p}{(\gamma-1)M_{N1}^2} - 1} = 0,$$

in which

$$p+2 = 2+(\gamma-1)M_1^2 = (M_{N1}^2-1)^2 (\gamma+1)^{\frac{1}{\gamma}} \Big/ \left[\left(\frac{p_{T2}}{p_{T1}} \right)^{\frac{\gamma-1}{\gamma}} (1+\gamma M_{N1}^2)^{\frac{\gamma+1}{\gamma}} - (\gamma+1)^{\frac{\gamma+1}{\gamma}} M_{N1}^2 \right] \quad \text{(C.4)}$$

This envelope condition reduces to the form

$$p^3 + C_1 p^2 + C_2 p + C_3 = 0,$$

in which

$$\left. \begin{aligned} C_1 &= 3 + \frac{1-(2\gamma^2-\gamma-2)M_{N1}^4}{(\gamma+1)M_{N1}^2} \\ C_2 &= -\frac{\gamma-1}{(\gamma+1)^2 M_{N1}^2} [M_{N1}^4 (6\gamma^2+(2\gamma+1)(M_{N1}^2+5))+(M_{N1}^2-1)] \\ C_3 &= \frac{2(\gamma-1)^2}{(\gamma+1)^2} (M_{N1}^2-1)[(2\gamma+1)M_{N1}^2+1]. \end{aligned} \right\} \quad \text{(C.5)}$$

Thus for a Chapman-Jouguet wave across which γ is constant, a chosen value of M_{N1} yields a particular cubic equation in p and, from the roots and equation (C.4), three possible combinations of p_{T2}/p_{T1} and M_1; of these three combinations, that corresponding to the larger of the two positive roots of the cubic gives the point on the envelope which corresponds to the value of M_{N1} originally chosen. Values of p_{T2}/p_{T1}, M_{N1}, M_1, δ, etc, which satisfy this envelope condition are listed in Table 5. It is seen that ζ hardly varies, being approximately 53°.

Table 1

Wave properties ($\gamma_1 = \gamma_2 = \gamma =$ constant)

	Wave properties in general form: $F = 1 + \sqrt{1 - \frac{2(\gamma+1)M_{N1}^2}{(M_{N1}^2-1)^2}\frac{q}{c_{p1}T_1}}$;	$A = \frac{F(M_{N1}^2-1)}{\gamma+1}$	Properties of Chapman-Jouguet detonations	Properties of shock waves
Static pressure ratio, p_2/p_1	$1 + \gamma F\frac{M_{N1}^2-1}{\gamma+1}$	$1+\gamma A$	$\frac{1+\gamma M_{N1}^2}{\gamma+1}$	$\frac{2\gamma M_{N1}^2-(\gamma-1)}{\gamma+1}$
Static density ratio, ρ_2/ρ_1 $(= u_1/u_2)$	$\frac{(\gamma+1)M_{N1}^2}{F+(\gamma+1-F)M_{N1}^2}$	$\frac{1}{1-(A/M_{N1}^2)}$	$\frac{(\gamma+1)M_{N1}^2}{1+\gamma M_{N1}^2}$	$\frac{(\gamma+1)M_{N1}^2}{2+(\gamma-1)M_{N1}^2}$
Static temperature ratio, T_2/T_1	$\frac{(\gamma+1+\gamma F(M_{N1}^2-1))(F+(\gamma+1-F)M_{N1}^2)}{(\gamma+1)^2M_{N1}^2}$	$(1+\gamma A)(1-(A/M_{N1}^2))$	$\frac{(1+\gamma M_{N1}^2)^2}{(\gamma+1)^2M_{N1}^2}$	$\frac{(2\gamma M_{N1}^2-(\gamma-1))(2+(\gamma-1)M_{N1}^2)}{(\gamma+1)^2M_{N1}^2}$
Normal Mach number ratio, M_{N2}/M_{N1}	$\sqrt{\frac{\gamma+1-[F(M_{N1}^2-1)/M_{N1}^2]}{\gamma+1+\gamma F(M_{N1}^2-1)}}$	$\sqrt{\frac{1-(A/M_{N1}^2)}{1+\gamma A}}$	$\frac{1}{M_{N1}}$ (i.e. $M_{N2}=1$)	$\sqrt{\frac{2+(\gamma-1)M_{N1}^2}{M_{N1}^2(2\gamma M_{N1}^2-(\gamma-1))}}$
Entropy rise, $e^{-\Delta s/R}$	$\left[\frac{\gamma+1}{\gamma+1+\gamma F(M_{N1}^2-1)}\right]^{\frac{1}{\gamma-1}}\left[\frac{(\gamma+1)M_{N1}^2}{F+(\gamma+1-F)M_{N1}^2}\right]^{\frac{\gamma}{\gamma-1}}$ (rows above: $f(\gamma,F,M_{N1})$)	$\frac{1}{(1+\gamma A)^{\frac{1}{\gamma-1}}(1-(A/M_{N1}^2))^{\frac{\gamma}{\gamma-1}}}$	$\left[\frac{\gamma+1}{1+\gamma M_{N1}^2}\right]^{\frac{\gamma+1}{\gamma-1}}M_{N1}^{\frac{2\gamma}{\gamma-1}}$	$\left[\frac{\gamma+1}{2\gamma M_{N1}^2-(\gamma-1)}\right]^{\frac{1}{\gamma-1}}\left[\frac{(\gamma+1)M_{N1}^2}{2+(\gamma-1)M_{N1}^2}\right]^{\frac{\gamma}{\gamma-1}}$
Stream velocity ratio, V_2/V_1	$\sqrt{1-\frac{F(M_{N1}^2-1)[2(\gamma+1)M_{N1}^2-F(M_{N1}^2-1)]}{(\gamma+1)^2M_{N1}^2M_1^2}}$	$\sqrt{\left(1-\frac{A}{M_1^2}\right)-\frac{A}{M_1^2}(1-(A/M_{N1}^2))}$	$\sqrt{1-\frac{(M_{N1}^2-1)(1+(2\gamma+1)M_{N1}^2)}{(\gamma+1)^2M_{N1}^2M_1^2}}$	$\sqrt{1-\frac{4(M_{N1}^2-1)(1+\gamma M_{N1}^2)}{(\gamma+1)^2M_{N1}^2M_1^2}}$
Stream Mach number ratio, M_2/M_1	$\sqrt{\frac{(\gamma+1)^2M_{N1}^2-F(M_{N1}^2-1)[2(\gamma+1)M_{N1}^2-F(M_{N1}^2-1)]/M_1^2}{(\gamma+1+\gamma F(M_{N1}^2-1))(F+(\gamma+1-F)M_{N1}^2)}}$	$\sqrt{\frac{\left(1-\frac{A}{M_1^2}\right)-\frac{A}{M_1^2}(1-(A/M_{N1}^2))}{(1+\gamma A)(1-(A/M_{N1}^2))M_1^2}}$	$\frac{1}{1+\gamma M_{N1}^2}\sqrt{(\gamma+1)^2M_{N1}^2-(M_{N1}^2-1)(1+(2\gamma+1)M_{N1}^2)/M_1^2}$	$\sqrt{\frac{(\gamma+1)^2M_{N1}^2-4(M_{N1}^2-1)(1+\gamma M_{N1}^2)/M_1^2}{(2\gamma M_{N1}^2-(\gamma-1))(2+(\gamma-1)M_{N1}^2)}}$
Stagnation temperature ratio, T_{T2}/T_{T1}	$1+\frac{F(2-F)(M_{N1}^2-1)^2}{(\gamma+1)M_{N1}^2(2+(\gamma-1)M_1^2)}$	Use of A produces little simplification	$1+\frac{(M_{N1}^2-1)^2}{(\gamma+1)M_{N1}^2(2+(\gamma-1)M_1^2)}$	1 (Therefore $p_{T2}/p_{T1} = e^{-\Delta s/R}$)
Stagnation pressure ratio, p_{T2}/p_{T1}	$\left[\frac{\gamma+1}{\gamma+1+\gamma F(M_{N1}^2-1)}\right]^{\frac{1}{\gamma-1}}\left[\frac{(\gamma+1)M_{N1}^2}{F+(\gamma+1-F)M_{N1}^2}+\frac{F(2-F)(M_{N1}^2-1)^2}{(F+(\gamma+1-F)M_{N1}^2)(2+(\gamma-1)M_1^2)}\right]^{\frac{\gamma}{\gamma-1}}$		$\left[\frac{\gamma+1}{1+\gamma M_{N1}^2}\right]^{\frac{\gamma+1}{\gamma-1}}\left[M_{N1}^2+\frac{(M_{N1}^2-1)^2}{(\gamma+1)(2+(\gamma-1)M_1^2)}\right]^{\frac{\gamma}{\gamma-1}}$	Identical with $e^{-\Delta s/R}$ Therefore $f(\gamma, M_{N1})$
Cotangent of deflection angle, $\cot\delta$	$\left[\frac{M_1^2(\gamma+1)}{F(M_{N1}^2-1)}-1\right]\Big/\sqrt{\left(\frac{M_1}{M_{N1}}\right)^2-1}$ (rows from stream velocity ratio: $f(\gamma,F,M_{N1},M_1)$)	$\left[\frac{M_1^2}{A}-1\right]\Big/\sqrt{\left(\frac{M_1}{M_{N1}}\right)^2-1}$	$\left[\frac{M_1^2(\gamma+1)}{M_{N1}^2-1}-1\right]\Big/\sqrt{\left(\frac{M_1}{M_{N1}}\right)^2-1}$	$\left[\frac{M_1^2(\gamma+1)}{2(M_{N1}^2-1)}-1\right]\Big/\sqrt{\left(\frac{M_1}{M_{N1}}\right)^2-1}$

TABLE 1

TABLE 2

Maximum flow deflection (M_{N1} constant, $\gamma = 1.4$, F = 1 and 2)

F = 1

M_{N1}	M_1	ζ	δ	M_{N1}	M_1	ζ	δ
1.0000	1.4142	45.0000	0.0000	4.1000	5.1993	52.0522	14.1043
1.0439	1.4636	45.5000	1.0000	4.2000	5.3242	52.0788	14.1576
1.0923	1.5185	46.0000	2.0000	4.3000	5.4491	52.1037	14.2074
1.1000	1.5273	46.0749	2.1499	4.4000	5.5740	52.1269	14.2538
1.1461	1.5800	46.5000	3.0000	4.5000	5.6990	52.1486	14.2973
1.2000	1.6422	46.9491	3.8983	4.6000	5.8241	52.1690	14.3380
1.2065	1.6497	47.0000	4.0000	4.7000	5.9492	52.1881	14.3762
1.2750	1.7293	47.5000	5.0000	4.7406	6.0000	52.1955	14.3910
1.3000	1.7586	47.6672	5.3343	4.8000	6.0743	52.2060	14.4120
1.3536	1.8215	48.0000	6.0000	4.9000	6.1994	52.2229	14.4458
1.4000	1.8762	48.2625	6.5250	5.0000	6.3246	52.2388	14.4775
1.4455	1.9301	48.5000	7.0000	5.1000	6.4497	52.2537	14.5074
1.5000	1.9948	48.7605	7.5210	5.2000	6.5750	52.2678	14.5357
1.5044	2.0000	48.7804	7.5608	5.3000	6.7002	52.2812	14.5624
1.5550	2.0603	49.0000	8.0000	5.4000	6.8254	52.2938	14.5876
1.6000	2.1142	49.1806	8.3612	5.5000	6.9507	52.3058	14.6115
1.6886	2.2207	49.5000	9.0000	5.5393	7.0000	52.3103	14.6206
1.7000	2.2344	49.5378	9.0755	5.6000	7.0760	52.3171	14.6342
1.8000	2.3551	49.8436	9.6872	5.7000	7.2013	52.3278	14.6556
1.8576	2.4249	50.0000	10.0000	5.8000	7.3267	52.3380	14.6760
1.9000	2.4764	50.1072	10.2145	5.9000	7.4520	52.3477	14.6954
2.0000	2.5981	50.3360	10.6719	6.0000	7.5774	52.3569	14.7138
2.0812	2.6972	50.5000	11.0000	6.1000	7.7028	52.3657	14.7314
2.1000	2.7201	50.5355	11.0711	6.2000	7.8282	52.3740	14.7481
2.2000	2.8425	50.7106	11.4212	6.3000	7.9536	52.3820	14.7640
2.3000	2.9652	50.8649	11.7299	6.3370	8.0000	52.3848	14.7697
2.3283	3.0000	50.9053	11.8107	6.4000	8.0790	52.3896	14.7792
2.3987	3.0865	51.0000	12.0000	6.5000	8.2044	52.3968	14.7937
2.4000	3.0881	51.0017	12.0034	6.6000	8.3299	52.4038	14.8075
2.5000	3.2113	51.1233	12.2467	6.7000	8.4553	52.4104	14.8208
2.6000	3.3347	51.2320	12.4641	6.8000	8.5808	52.4167	14.8334
2.7000	3.4582	51.3295	12.6590	6.9000	8.7063	52.4228	14.8456
2.8000	3.5819	51.4172	12.8345	7.0000	8.8318	52.4286	14.8572
2.9000	3.7057	51.4965	12.9930	7.1000	8.9573	52.4341	14.8683
2.9047	3.7115	51.5000	13.0000	7.1341	9.0000	52.4360	14.8720
3.0000	3.8297	51.5683	13.1366	7.2000	9.0828	52.4395	14.8790
3.1000	3.9538	51.6335	13.2670	7.3000	9.2083	52.4446	14.8892
3.1372	4.0000	51.6563	13.3126	7.4000	9.3338	52.4495	14.8990
3.2000	4.0780	51.6930	13.3859	7.5000	9.4593	52.4542	14.9085
~~3.3000~~	~~4.2025~~	~~51.7473~~	~~13.4946~~	7.6000	9.5849	52.4588	14.9176
3.4000	4.3267	51.7971	13.5941	7.7000	9.7104	52.4631	14.9263
3.5000	4.4511	51.8428	13.6855	7.8000	9.8360	52.4673	14.9347
3.6000	4.5757	51.8848	13.7697	7.9000	9.9616	52.4714	14.9428
3.7000	4.7003	51.9236	13.8473	7.9306	10.0000	52.4726	14.9452
3.8000	4.8249	51.9595	13.9190	8.0000	10.0871	52.4753	14.9505
3.9000	4.9497	51.9927	13.9854				
3.9230	4.9784	52.0000	14.0000				
3.9403	5.0000	52.0054	14.0108				
4.0000	5.0744	52.0235	14.0470				

F = 2

M_{N1}	M_1	ζ	δ	M_{N1}	M_1	ζ	δ
1.0000	1.4142	45.0000	0.0000	3.1000	3.4706	63.2807	36.5613
1.0212	1.4318	45.5000	1.0000	3.1895	3.5639	63.5000	37.0000
1.0431	1.4501	46.0000	2.0000	3.2000	3.5749	63.5247	37.0494
1.0656	1.4691	46.5000	3.0000	3.3000	3.6794	63.7501	37.5003
1.0888	1.4888	47.0000	4.0000	3.4000	3.7842	63.9587	37.9174
1.1000	1.4983	47.2354	4.4708	3.4207	3.8059	64.0000	38.0000
1.1128	1.5093	47.5000	5.0000	3.5000	3.8891	64.1520	38.3041
1.1375	1.5306	48.0000	6.0000	3.6000	3.9942	64.3315	38.6630
1.1630	1.5529	48.5000	7.0000	3.6056	4.0000	64.3411	38.6822
1.1895	1.5761	49.0000	8.0000	3.7000	4.0994	64.4984	38.9968
1.2000	1.5853	49.1944	8.3887	3.7010	4.1004	64.5000	39.0000
1.2169	1.6003	49.5000	9.0000	3.8000	4.2048	64.6538	39.3076
1.2452	1.6255	50.0000	10.0000	3.9000	4.3103	64.7988	39.5976
1.2747	1.6520	50.5000	11.0000	4.0000	4.4159	64.9342	39.8683
1.3000	1.6748	50.9145	11.8290	4.0512	4.4700	65.0000	40.0000
1.3053	1.6796	51.0000	12.0000	4.1000	4.5216	65.0608	40.1216
1.3372	1.7086	51.5000	13.0000	4.2000	4.6275	65.1794	40.3588
1.3704	1.7391	52.0000	14.0000	4.3000	4.7334	65.2906	40.5812
1.4000	1.7664	52.4286	14.8572	4.4000	4.8394	65.3950	40.7899
1.4050	1.7710	52.5000	15.0000	4.5000	4.9455	65.4931	40.9862
1.4413	1.8046	53.0000	16.0000	4.5073	4.9532	65.5000	41.0000
1.4792	1.8401	53.5000	17.0000	4.6000	5.0517	65.5854	41.1709
1.5000	1.8597	53.7650	17.5300	4.7000	5.1580	65.6724	41.3449
1.5189	1.8775	54.0000	18.0000	4.8000	5.2643	65.7545	41.5090
1.5607	1.9171	54.5000	19.0000	4.9000	5.3708	65.8320	41.6639
1.6000	1.9545	54.9480	19.8960	5.0000	5.4772	65.9052	41.8103
1.6047	1.9590	55.0000	20.0000	5.1000	5.5838	65.9744	41.9488
1.6475	2.0000	55.4624	20.9248	5.1384	5.6247	66.0000	42.0000
1.6511	2.0034	55.5000	21.0000	5.2000	5.6903	66.0400	42.0799
1.7000	2.0506	55.9984	21.9968	5.3000	5.7970	66.1021	42.2042
1.7002	2.0508	56.0000	22.0000	5.4000	5.9037	66.1610	42.3221
1.7522	2.1012	56.5000	23.0000	5.4903	6.0000	66.2117	42.4233
1.8000	2.1479	56.9338	23.8676	5.5000	6.0104	66.2170	42.4340
1.8075	2.1552	57.0000	24.0000	5.6000	6.1172	66.2702	42.5403
1.8665	2.2131	57.5000	25.0000	5.7000	6.2240	66.3207	42.6414
1.9000	2.2461	57.7693	25.5387	5.8000	6.3309	66.3688	42.7377
1.9297	2.2754	58.0000	26.0000	5.9000	6.4378	66.4147	42.8293
1.9975	2.3427	58.5000	27.0000	6.0000	6.5447	66.4583	42.9167
2.0000	2.3452	58.5178	27.0357	6.1000	6.6517	66.5000	43.0000
2.0706	2.4156	59.0000	28.0000	6.2000	6.7587	66.5397	43.0795
2.1000	2.4451	59.1903	28.3807	6.3000	6.8657	66.5777	43.1554
2.1498	2.4951	59.5000	29.0000	6.4000	6.9728	66.6140	43.2280
2.2000	2.5456	59.7962	29.5924	6.4254	7.0000	66.6230	43.2459
2.2361	2.5820	60.0000	30.0000	6.5000	7.0799	66.6487	43.2974
2.3000	2.6467	60.3436	30.6871	6.6000	7.1870	66.6819	43.3638
2.3305	2.6777	60.5000	31.0000	6.7000	7.2942	66.7137	43.4274
2.4000	2.7483	60.8393	31.6786	6.8000	7.4014	66.7442	43.4884
2.4346	2.7836	61.0000	32.0000	6.9000	7.5086	66.7734	43.5468
2.5000	2.8504	61.2895	32.5790	7.0000	7.6158	66.8014	43.6028
2.5502	2.9019	61.5000	33.0000	7.1000	7.7230	66.8283	43.6566
2.6000	2.9530	61.6992	33.3985	7.2000	7.8303	66.8541	43.7082
2.6458	3.0000	61.8745	33.7490	7.3000	7.9376	66.8789	43.7578
2.6797	3.0350	62.0000	34.0000	7.3582	8.0000	66.8929	43.7858
2.7000	3.0559	62.0731	34.1462	7.4000	8.0449	66.9028	43.8055
2.8000	3.1591	62.4150	34.8299	7.5000	8.1522	66.9257	43.8514
2.8263	3.1863	62.5000	35.0000	7.6000	8.2595	66.9477	43.8955
2.9000	3.2627	62.7282	35.4565	7.7000	8.3669	66.9690	43.9380
2.9942	3.3605	63.0000	36.0000	7.8000	8.4743	66.9894	43.9789
3.0000	3.3665	63.0159	36.0319	7.8532	8.5314	67.0000	44.0000
				7.9000	8.5817	67.0091	44.0183
				8.0000	8.6891	67.0281	44.0563

TABLE 3

Maximum flow deflection (M_1 constant, γ = 1.4, F = 1 and 2)

M_{N1}	M_1	ζ	δ
1.0000	1.0000	90.0000	0.0000
1.0003	1.0005	89.0000	0.0003
1.0012	1.0018	88.0000	0.0020
1.0028	1.0041	87.0000	0.0069
1.0049	1.0074	86.0000	0.0163
1.0077	1.0116	85.0000	0.0319
1.0112	1.0168	84.0000	0.0552
1.0154	1.0230	83.0000	0.0879
1.0203	1.0303	82.0000	0.1317
1.0260	1.0387	81.0000	0.1881
1.0324	1.0484	80.0000	0.2590
1.0398	1.0593	79.0000	0.3461
1.0481	1.0715	78.0000	0.4514
1.0574	1.0852	77.0000	0.5767
1.0678	1.1005	76.0000	0.7241
1.0795	1.1175	75.0000	0.8955
1.0864	1.1276	74.4543	1.0000
1.0924	1.1365	74.0000	1.0932
1.1000	1.1475	73.4637	1.2108
1.1069	1.1575	73.0000	1.3193
1.1231	1.1809	72.0000	1.5761
1.1411	1.2069	71.0000	1.8660
1.1495	1.2188	70.5742	2.0000
1.1613	1.2359	70.0000	2.1913
1.1840	1.2683	69.0000	2.5544
1.2000	1.2910	68.3619	2.8071
1.2096	1.3046	68.0000	2.9579
1.2123	1.3084	67.9013	3.0000
1.2386	1.3455	67.0000	3.4041
1.2715	1.3918	66.0000	3.8954
1.2787	1.4019	65.7987	4.0000
1.3000	1.4317	65.2325	4.3046
1.3093	1.4446	65.0000	4.4342
1.3511	1.5028	64.0367	5.0000
1.3528	1.5052	64.0000	5.0224
1.4000	1.5703	63.0662	5.6181
1.4036	1.5753	63.0000	5.6621
1.4321	1.6145	62.5026	5.9999
1.4635	1.6576	62.0000	6.3547
1.5000	1.7074	61.4681	6.7450
1.5250	1.7414	61.1314	7.0001
1.5352	1.7553	61.0000	7.1012
1.6000	1.8431	60.2397	7.7053
1.6226	1.8737	60.0000	7.9022
1.6342	1.8893	59.8823	8.0000
1.7000	1.9778	59.2672	8.5234
1.7166	2.0000	59.1253	8.6470
1.7317	2.0203	59.0000	8.7570
1.7665	2.0668	58.7266	9.0000
1.8000	2.1115	58.4799	9.2226
1.8722	2.2076	58.0000	9.6645
1.9000	2.2446	57.8312	9.8227
1.9326	2.2878	57.6439	10.0000
2.0000	2.3770	57.2889	10.3405
2.0611	2.4575	57.0000	10.6221
2.1000	2.5088	56.8300	10.7895
2.1521	2.5773	56.6182	11.0001
2.2000	2.6402	56.4377	11.1810
2.3000	2.7711	56.0992	11.5241
2.3322	2.8131	56.0000	11.6256
2.4000	2.9016	55.8049	11.8263
2.4636	2.9844	55.6372	11.9999
2.4756	3.0000	55.6072	12.0312
2.5000	3.0318	55.5472	12.0936
2.6000	3.1617	55.3202	12.3312
2.7000	3.2913	55.1191	12.5432
2.7652	3.3757	55.0000	12.6694
2.8000	3.4207	54.9400	12.7331
2.9000	3.5498	54.7798	12.9039
2.9611	3.6287	54.6900	12.9999
3.0000	3.6788	54.6359	13.0580
3.1000	3.8075	54.5061	13.1975
3.2000	3.9361	54.3886	13.3243
3.2497	4.0000	54.3342	13.3830
3.3000	4.0645	54.2819	13.4397
3.4000	4.1928	54.1846	13.5451
3.5000	4.3210	54.0958	13.6416
3.6000	4.4490	54.0144	13.7302
3.6186	4.4729	54.0000	13.7459
3.7000	4.5770	53.9397	13.8117
3.8000	4.7048	53.8708	13.8869
3.9000	4.8325	53.8073	13.9563
3.9670	4.9180	53.7674	14.0000
4.0000	4.9601	53.7485	14.0207
4.0312	5.0000	53.7311	14.0398
4.1000	5.0877	53.6941	14.0803
4.2000	5.2152	53.6435	14.1358
4.3000	5.3426	53.5965	14.1874
4.4000	5.4699	53.5527	14.2356
4.5000	5.5972	53.5118	14.2806
4.6000	5.7244	53.4736	14.3226
4.7000	5.8515	53.4378	14.3620
4.8000	5.9786	53.4042	14.3990
4.8168	6.0000	53.3988	14.4050
4.9000	6.1057	53.3727	14.4337
5.0000	6.2327	53.3431	14.4664
5.1000	6.3596	53.3152	14.4972
5.2000	6.4865	53.2889	14.5262
5.3000	6.6134	53.2641	14.5535
5.4000	6.7403	53.2407	14.5794
5.5000	6.8671	53.2185	14.6039
5.6000	6.9938	53.1976	14.6270
5.6049	7.0000	53.1966	14.6281
5.7000	7.1206	53.1777	14.6490
5.8000	7.2473	53.1589	14.6698
5.9000	7.3740	53.1410	14.6896
6.0000	7.5006	53.1240	14.7084
6.1000	7.6272	53.1078	14.7263
6.2000	7.7538	53.0924	14.7433
6.3000	7.8804	53.0778	14.7595
6.3945	8.0000	53.0646	14.7741
6.4000	8.0070	53.0638	14.7750
6.5000	8.1335	53.0505	14.7897
6.6000	8.2600	53.0378	14.8038
6.7000	8.3865	53.0256	14.8172
6.8000	8.5130	53.0140	14.8301
6.9000	8.6394	53.0029	14.8424
6.9267	8.6732	53.0000	14.8456
7.0000	8.7658	52.9923	14.8542
7.1000	8.8923	52.9821	14.8655
7.1852	9.0000	52.9737	14.8748
7.2000	9.0187	52.9723	14.8763
7.3000	9.1451	52.9629	14.8867
7.4000	9.2714	52.9539	14.8967
7.5000	9.3978	52.9453	14.9062
7.6000	9.5241	52.9370	14.9154
7.7000	9.6505	52.9290	14.9243
7.8000	9.7768	52.9214	14.9328
7.9000	9.9031	52.9140	14.9409
7.9767	10.0000	52.9085	14.9470
8.0000	10.0294	52.9069	14.9488

TABLE 3—*continued*

M_{N1}	M_1	ζ	δ
1.0000	1.0000	90.0000	0.0000
1.0003	1.0005	88.9998	0.0005
1.0012	1.0018	87.9999	0.0041
1.0028	1.0041	86.9999	0.0138
1.0049	1.0074	85.9999	0.0329
1.0078	1.0116	85.0000	0.0646
1.0113	1.0169	84.0000	0.1126
1.0156	1.0232	83.0000	0.1805
1.0206	1.0307	82.0000	0.2725
1.0266	1.0393	81.0000	0.3930
1.0334	1.0493	80.0000	0.5472
1.0412	1.0607	79.0000	0.7407
1.0503	1.0737	78.0000	0.9799
1.0510	1.0748	77.9247	1.0000
1.0606	1.0885	77.0000	1.2726
1.0724	1.1052	76.0000	1.6275
1.0842	1.1218	75.1196	2.0000
1.0859	1.1242	75.0000	2.0554
1.1000	1.1438	74.0874	2.5206
1.1015	1.1458	74.0000	2.5694
1.1141	1.1633	73.2825	3.0000
1.1195	1.1706	73.0000	3.1856
1.1406	1.1993	72.0000	3.9252
1.1427	1.2021	71.9083	4.0001
1.1655	1.2327	71.0000	4.8156
1.1706	1.2395	70.8147	5.0000
1.1955	1.2722	70.0000	5.8952
1.1984	1.2760	69.9127	6.0000
1.2000	1.2781	69.8660	6.0569
1.2263	1.3122	69.1516	7.0000
1.2324	1.3201	69.0000	7.2195
1.2544	1.3483	68.4993	8.0000
1.2795	1.3800	67.9998	8.8767
1.2830	1.3844	67.9343	9.0000
1.3000	1.4057	67.6387	9.5833
1.3123	1.4210	67.4413	10.0000
1.3422	1.4580	67.0089	11.0000
1.3429	1.4588	67.0000	11.0219
1.3730	1.4957	66.6287	12.0000
1.4000	1.5285	66.3409	12.8523
1.4048	1.5342	66.2941	13.0000
1.4376	1.5737	66.0000	13.9996
1.4376	1.5737	65.9999	14.0000
1.4717	1.6143	65.7418	15.0000
1.5000	1.6476	65.5591	15.7995
1.5072	1.6562	65.5164	16.0000
1.5442	1.6995	65.3209	17.0000
1.5829	1.7444	65.1530	18.0000
1.6000	1.7641	65.0893	18.4261
1.6235	1.7912	65.0107	19.0000
1.6270	1.7952	65.0000	19.0826
1.6662	1.8400	64.8923	20.0000
1.7000	1.8785	64.8177	20.7570
1.7112	1.8912	64.7964	21.0000
1.7587	1.9449	64.7220	22.0000
1.8000	1.9914	64.6759	22.8243
1.8077	2.0000	64.6690	22.9735
1.8091	2.0015	64.6678	23.0000
1.8627	2.0614	64.6331	24.0000
1.9000	2.1030	64.6205	24.6602
1.9199	2.1250	64.6171	25.0000
1.9811	2.1928	64.6191	26.0000
2.0000	2.2136	64.6231	26.2942
2.0470	2.2653	64.6386	27.0000
2.1000	2.3235	64.6646	27.7529
2.1181	2.3433	64.6751	28.0000
2.1953	2.4276	64.7282	29.0000
2.2000	2.4328	64.7319	29.0588
2.2794	2.5192	64.7975	30.0000
2.3000	2.5416	64.8158	30.2316
2.3717	2.6194	64.8827	31.0000
2.4000	2.6500	64.9101	31.2882
2.4736	2.7297	64.9834	32.0000
2.5000	2.7582	65.0102	32.2428
2.5870	2.8521	65.0994	32.9999
2.6000	2.8662	65.1129	33.1078
2.7000	2.9739	65.2160	33.8938
2.7143	2.9893	65.2306	34.0000
2.7242	3.0000	65.2408	34.0734
2.8000	3.0815	65.3180	34.6099
2.8586	3.1445	65.3767	35.0000
2.9000	3.1890	65.4177	35.2640
3.0000	3.2965	65.5145	35.8626
3.0242	3.3224	65.5375	36.0000
3.1000	3.4038	65.6080	36.4122
3.2000	3.5111	65.6978	36.9175
3.2171	3.5295	65.7128	37.0000
3.3000	3.6184	65.7837	37.3832
3.4000	3.7257	65.8659	37.8132
3.4460	3.7750	65.9024	38.0000
3.5000	3.8329	65.9443	38.2109
3.6000	3.9401	66.0189	38.5796
3.6559	4.0000	66.0590	38.7739
3.7000	4.0473	66.0899	38.9219
3.7239	4.0729	66.1063	39.0000
3.8000	4.1546	66.1574	39.2402
3.9000	4.2618	66.2215	39.5366
4.0000	4.3690	66.2825	39.8132
4.0716	4.4458	66.3242	40.0000
4.1000	4.4762	66.3404	40.0716
4.2000	4.5835	66.3954	40.3133
4.3000	4.6908	66.4476	40.5397
4.4000	4.7980	66.4973	40.7521
4.5000	4.9053	66.5445	40.9516
4.5252	4.9324	66.5561	41.0000
4.5882	5.0000	66.5842	41.1177
4.6000	5.0126	66.5894	41.1392
4.7000	5.1200	66.6321	41.3168
4.8000	5.2273	66.6728	41.4822
4.9000	5.3346	66.7115	41.6392
5.0000	5.4420	66.7483	41.7875
5.1000	5.5494	66.7834	41.9277
5.1538	5.6072	66.8016	42.0000
5.2000	5.6568	66.8169	42.0604
5.3000	5.7642	66.8488	42.1861
5.4000	5.8716	66.8793	42.3053
5.5000	5.9790	66.9084	42.4184
5.5195	6.0000	66.9139	42.4398
5.6000	6.0865	66.9362	42.5258
5.7000	6.1940	66.9628	42.6279
5.8000	6.3014	66.9882	42.7251
5.9000	6.4089	67.0125	42.8175
6.0000	6.5164	67.0357	42.9056
6.1000	6.6240	67.0580	42.9896
6.1127	6.6376	67.0608	43.0000
6.2000	6.7315	67.0794	43.0698
6.3000	6.8390	67.0998	43.1464
6.4000	6.9466	67.1195	43.2195
6.4497	7.0000	67.1289	43.2546
6.5000	7.0541	67.1383	43.2894
6.6000	7.1617	67.1564	43.3563
6.7000	7.2693	67.1737	43.4203
6.8000	7.3769	67.1904	43.4817
6.9000	7.4845	67.2064	43.5405
7.0000	7.5921	67.2219	43.5969
7.1000	7.6997	67.2367	43.6510
7.2000	7.8074	67.2510	43.7029
7.3000	7.9150	67.2647	43.7528
7.3790	8.0000	67.2752	43.7908
7.4000	8.0226	67.2780	43.8007
7.5000	8.1303	67.2907	43.8468
7.6000	8.2380	67.3030	43.8912
7.7000	8.3456	67.3149	43.9339
7.8000	8.4533	67.3264	43.9750
7.8627	8.5208	67.3333	44.0000
7.9000	8.5610	67.3374	44.0146
8.0000	8.6687	67.3481	44.0528

TABLE 4

Absolute maximum flow deflection and corresponding wave angle

(γ = 1.4, F = 1 (0.01)2)

F	δ	ζ	F	δ	ζ
1.0000	15.2575	52.6288	1.5100	27.3204	58.6602
1.0100	15.4556	52.7278	1.5200	27.6077	58.8038
1.0200	15.6548	52.8274	1.5300	27.8974	58.9487
1.0300	15.8553	52.9277	1.5400	28.1897	59.0949
1.0400	16.0571	53.0286	1.5500	28.4846	59.2423
1.0500	16.2602	53.1301	1.5600	28.7822	59.3911
1.0600	16.4646	53.2323	1.5700	29.0825	59.5412
1.0700	16.6703	53.3351	1.5800	29.3855	59.6928
1.0800	16.8773	53.4386	1.5900	29.6913	59.8457
1.0900	17.0856	53.5428	1.6000	30.0000	60.0000
1.1000	17.2953	53.6477	1.6100	30.3116	60.1558
1.1100	17.5064	53.7532	1.6200	30.6261	60.3131
1.1200	17.7189	53.8595	1.6300	30.9437	60.4719
1.1300	17.9328	53.9664	1.6400	31.2643	60.6322
1.1400	18.1482	54.0741	1.6500	31.5881	60.7941
1.1500	18.3649	54.1825	1.6600	31.9151	60.9576
1.1600	18.5832	54.2916	1.6700	32.2454	61.1237
1.1700	18.8029	54.4015	1.6800	32.5790	61.2895
1.1800	19.0242	54.5121	1.6900	32.9160	61.4580
1.1900	19.2469	54.6235	1.7000	33.2564	61.6282
1.2000	19.4712	54.7356	1.7100	33.6004	61.8002
1.2100	19.6971	54.8485	1.7200	33.9481	61.9740
1.2200	19.9245	54.9623	1.7300	34.2994	62.1497
1.2300	20.1536	55.0768	1.7400	34.6546	62.3273
1.2400	20.3843	55.1921	1.7500	35.0136	62.5068
1.2500	20.6166	55.3083	1.7600	35.3765	62.6883
1.2600	20.8506	55.4253	1.7700	35.7436	62.8718
1.2700	21.0863	55.5431	1.7800	36.1147	63.0574
1.2800	21.3237	55.6618	1.7900	36.4901	63.2451
1.2900	21.5628	55.7814	1.8000	36.8699	63.4349
1.3000	21.8037	55.9019	1.8100	37.2541	63.6271
1.3100	22.0465	56.0232	1.8200	37.6429	63.8215
1.3200	22.2910	56.1455	1.8300	38.0364	64.0182
1.3300	22.5373	56.2687	1.8400	38.4347	64.2173
1.3400	22.7856	56.3928	1.8500	38.8379	64.4189
1.3500	23.0357	56.5178	1.8600	39.2461	64.6231
1.3600	23.2877	56.6439	1.8700	39.6596	64.8298
1.3700	23.5417	56.7709	1.8800	40.0734	65.0392
1.3800	23.7977	56.8989	1.8900	40.5027	65.2514
1.3900	24.0557	57.0279	1.9000	40.9327	65.4664
1.4000	24.3157	57.1579	1.9100	41.3685	65.6843
1.4100	24.5778	57.2889	1.9200	41.8103	65.9052
1.4200	24.8421	57.4210	1.9300	42.2583	66.1291
1.4300	25.1084	57.5542	1.9400	42.7126	66.3563
1.4400	25.3769	57.6885	1.9500	43.1735	66.5868
1.4500	25.6477	57.8238	1.9600	43.6413	66.8206
1.4600	25.9206	57.9603	1.9700	44.1160	67.0580
1.4700	26.1959	58.0979	1.9800	44.5980	67.2990
1.4800	26.4735	58.2367	1.9900	45.0874	67.5437
1.4900	26.7534	58.3767	2.0000	45.5847	67.7923
1.5000	27.0357	58.5178			

TABLE 5

Wave properties on envelope of Fig. 13 (γ = 1.4, F = 1)

M_{N1}	p	M_1	V_2/V_1	T_{T2}/T_{T1}	M_2	p_{T2}/p_{T1}	ζ	δ
1.0000	0.6271	1.2521	1.0000	1.0000	1.2521	1.0000	53.0019	0.0000
1.0223	0.6545	1.2791	0.9886	1.0003	1.2596	9.9965, -1	53.0530	0.5000
1.0394	0.6760	1.3000	0.9803	1.0009	1.2653	9.9892, -1	53.0894	0.8709
1.0456	0.6838	1.3074	0.9774	1.0012	1.2673	9.9856, -1	53.1017	1.0000
1.0700	0.7152	1.3372	0.9656	1.0028	1.2752	9.9660, -1	53.1490	1.5000
1.0956	0.7490	1.3684	0.9560	1.0051	1.2833	9.9367, -1	53.1917	2.0000
1.1215	0.7840	1.4000	0.9461	1.0079	1.2913	9.8983, -1	53.2312	2.4804
1.1000	0.7549	1.3738	0.9543	1.0055	1.2847	9.9309, -1	53.1987	2.0831
1.1226	0.7855	1.4013	0.9457	1.0080	1.2917	9.8965, -1	53.2327	2.5000
1.1510	0.8250	1.4361	0.9357	1.0117	1.3003	9.8437, -1	53.2709	3.0000
1.1811	0.8678	1.4730	0.9259	1.0162	1.3091	9.7769, -1	53.3062	3.5000
1.2031	0.9000	1.5000	0.9192	1.0199	1.3155	9.7209, -1	53.3289	3.8487
1.2000	0.8954	1.4962	0.9201	1.0193	1.3146	9.7292, -1	53.3259	3.8005
1.2129	0.9145	1.5121	0.9164	1.0216	1.3183	9.6941, -1	53.3383	4.0000
1.2468	0.9656	1.5537	0.9071	1.0278	1.3277	9.5933, -1	53.3671	4.5000
1.2829	1.0217	1.5982	0.8981	1.0349	1.3374	9.4723, -1	53.3925	5.0000
1.2844	1.0240	1.6000	0.8977	1.0353	1.3378	9.4671, -1	53.3934	5.0199
1.3000	1.0488	1.6192	0.8941	1.0385	1.3419	9.4105, -1	53.4028	5.2254
1.3215	1.0835	1.6458	0.8893	1.0431	1.3474	9.3285, -1	53.4142	5.5000
1.3630	1.1521	1.6971	0.8807	1.0524	1.3578	9.1590, -1	53.4321	6.0000
1.3653	1.1560	1.7000	0.8803	1.0529	1.3584	9.1491, -1	53.4330	6.0269
1.4000	1.2150	1.7429	0.8738	1.0609	1.3667	8.9963, -1	53.4439	6.4158
1.4078	1.2285	1.7525	0.8724	1.0628	1.3685	8.9608, -1	53.4459	6.5000
1.4461	1.2959	1.8000	0.8660	1.0720	1.3773	8.7801, -1	53.4538	6.8981
1.4563	1.3143	1.8126	0.8643	1.0745	1.3796	8.7304, -1	53.4554	7.0000
1.5091	1.4111	1.8782	0.8565	1.0875	1.3911	8.4641, -1	53.4603	7.5000
1.5265	1.4440	1.9000	0.8541	1.0919	1.3948	8.3729, -1	53.4609	7.6561
1.5000	1.3942	1.8670	0.8578	1.0852	1.3892	8.5108, -1	53.4598	7.4172
1.5669	1.5214	1.9503	0.8488	1.1021	1.4030	8.1579, -1	53.4604	8.0000
1.6068	1.5999	2.0000	0.8441	1.1122	1.4108	7.9403, -1	53.4577	8.3183
1.6000	1.5864	1.9915	0.8449	1.1104	1.4095	7.9777, -1	53.4583	8.2654
1.6307	1.6481	2.0298	0.8414	1.1183	1.4153	7.8076, -1	53.4552	8.5000
1.6869	1.7640	2.1000	0.8357	1.1325	1.4255	7.4924, -1	53.4472	8.9005
1.7000	1.7915	2.1163	0.8344	1.1358	1.4278	7.4187, -1	53.4449	8.9887
1.7017	1.7951	2.1184	0.8343	1.1363	1.4281	7.4091, -1	53.4446	9.0000
1.7669	1.9360	2.2000	0.8285	1.1527	1.4391	7.0395, -1	53.4314	9.4140
1.7813	1.9678	2.2180	0.8273	1.1563	1.4414	6.9580, -1	53.4281	9.5000
1.8457	2.1160	2.3000	0.8223	1.1725	1.4516	6.5889, -1	53.4119	9.8694
1.8000	2.0096	2.2414	0.8258	1.1609	1.4444	6.8521, -1	53.4237	9.6093
1.8715	2.1734	2.3310	0.8206	1.1785	1.4553	6.4508, -1	53.4053	10.0000
1.9265	2.3040	2.4000	0.8170	1.1918	1.4631	6.1470, -1	53.3899	10.2747
1.9000	2.2406	2.3667	0.8187	1.1854	1.4594	6.2926, -1	53.3974	10.1451
1.9750	2.4224	2.4609	0.8141	1.2032	1.4697	5.8844, -1	53.3757	10.5000
2.0062	2.5000	2.5000	0.8123	1.2105	1.4738	5.7189, -1	53.3664	10.6369
2.0000	2.4845	2.4923	0.8126	1.2091	1.4730	5.7514, -1	53.3682	10.6103
2.0858	2.7040	2.6000	0.8082	1.2285	1.4836	5.3078, -1	53.3420	10.9618
2.0957	2.7301	2.6125	0.8078	1.2308	1.4848	5.2578, -1	53.3389	11.0000
2.1652	2.9159	2.7000	0.8047	1.2459	1.4927	4.9167, -1	53.3172	11.2541
2.1000	2.7414	2.6179	0.8076	1.2317	1.4853	5.2362, -1	53.3375	11.0164
2.2000	3.0111	2.7437	0.8032	1.2533	1.4964	4.7523, -1	53.3064	11.3728
2.2390	3.1198	2.7928	0.8017	1.2615	1.5005	4.5727, -1	53.2943	11.5000
2.2447	3.1360	2.8000	0.8015	1.2626	1.5011	4.5467, -1	53.2925	11.5183
2.3000	3.2937	2.8696	0.7995	1.2738	1.5065	4.3025, -1	53.2754	11.6871
2.3242	3.3639	2.9000	0.7987	1.2786	1.5088	4.1991, -1	53.2680	11.7574
2.4000	3.5892	2.9955	0.7963	1.2932	1.5158	3.8879, -1	53.2451	11.9654
2.4035	3.5999	3.0000	0.7962	1.2939	1.5161	3.8738, -1	53.2441	11.9747
2.4133	3.6295	3.0123	0.7959	1.2957	1.5169	3.8354, -1	53.2412	12.0000
2.4829	3.8439	3.1000	0.7939	1.3085	1.5228	3.5707, -1	53.2208	12.1726
2.5000	3.8975	3.1215	0.7935	1.3116	1.5242	3.5083, -1	53.2158	12.2130
2.5622	4.0959	3.2000	0.7919	1.3224	1.5290	3.2892, -1	53.1982	12.3535
2.6000	4.2186	3.2476	0.7910	1.3288	1.5318	3.1627, -1	53.1877	12.4341
2.6320	4.3243	3.2880	0.7903	1.3342	1.5342	3.0588, -1	53.1789	12.5000
2.6416	4.3560	3.3000	0.7901	1.3357	1.5348	3.0285, -1	53.1763	12.5192
2.7000	4.5526	3.3736	0.7888	1.3451	1.5389	2.8494, -1	53.1608	12.6324

TABLE 5—*continued*

2.7209	4.6240	3.4000	0.7884	1.3484	1.5403	2.7878,	-1	53.1554	12.6712
2.8000	4.8993	3.4998	0.7869	1.3604	1.5453	2.5664,	-1	53.1353	12.8107
2.8001	4.8999	3.5000	0.7869	1.3604	1.5453	2.5660,	-1	53.1353	12.8110
2.8795	5.1841	3.6000	0.7855	1.3719	1.5501	2.3616,	-1	53.1160	12.9400
2.9000	5.2589	3.6259	0.7852	1.3748	1.5512	2.3115,	-1	53.1111	12.9717
2.9187	5.3273	3.6494	0.7849	1.3773	1.5523	2.2669,	-1	53.1067	13.0000
2.9587	5.4759	3.7000	0.7843	1.3828	1.5545	2.1740,	-1	53.0975	13.0590
3.0000	5.6312	3.7521	0.7837	1.3883	1.5567	2.0823,	-1	53.0882	13.1175
3.0380	5.7760	3.8000	0.7831	1.3932	1.5586	2.0015,	-1	53.0799	13.1693
3.1000	6.0162	3.8782	0.7823	1.4010	1.5617	1.8766,	-1	53.0666	13.2499
3.1172	6.0840	3.9000	0.7821	1.4031	1.5625	1.8433,	-1	53.0630	13.2715
3.1965	6.3999	4.0000	0.7811	1.4125	1.5662	1.6982,	-1	53.0470	13.3665
3.2000	6.4141	4.0044	0.7811	1.4129	1.5663	1.6921,	-1	53.0463	13.3706
3.2757	6.7239	4.1000	0.7802	1.4214	1.5696	1.5652,	-1	53.0316	13.4549
3.3000	6.8247	4.1306	0.7800	1.4241	1.5706	1.5267,	-1	53.0271	13.4807
3.3184	6.9016	4.1538	0.7798	1.4261	1.5713	1.4983,	-1	53.0237	13.5000
3.3550	7.0559	4.2000	0.7794	1.4300	1.5728	1.4433,	-1	53.0170	13.5373
3.4000	7.2480	4.2568	0.7790	1.4346	1.5746	1.3787,	-1	53.0090	13.5816
3.4342	7.3959	4.3000	0.7786	1.4381	1.5758	1.3316,	-1	53.0031	13.6142
3.5000	7.6840	4.3829	0.7780	1.4445	1.5782	1.2460,	-1	52.9920	13.6742
3.5135	7.7439	4.4000	0.7779	1.4458	1.5787	1.2292,	-1	52.9898	13.6861
3.5927	8.0999	4.5000	0.7773	1.4532	1.5814	1.1354,	-1	52.9771	13.7535
3.6000	8.1328	4.5091	0.7772	1.4539	1.5816	1.1272,	-1	52.9760	13.7594
3.6720	8.4639	4.6000	0.7767	1.4602	1.5840	1.0494,	-1	52.9650	13.8166
3.7000	8.5944	4.6353	0.7764	1.4626	1.5848	1.0208,	-1	52.9609	13.8379
3.7512	8.8358	4.7000	0.7761	1.4669	1.5864	9.7058,	-2	52.9535	13.8758
3.8000	9.0686	4.7615	0.7757	1.4709	1.5878	9.2536,	-2	52.9467	13.9105
3.8305	9.2160	4.8000	0.7755	1.4733	1.5886	8.9822,	-2	52.9425	13.9316
3.9000	9.5555	4.8876	0.7751	1.4787	1.5905	8.3978,	-2	52.9332	13.9777
3.9098	9.6040	4.9000	0.7750	1.4794	1.5908	8.3188,	-2	52.9320	13.9840
3.9350	9.7290	4.9318	0.7749	1.4813	1.5915	8.1195,	-2	52.9287	14.0000
3.9891	9.9999	5.0000	0.7746	1.4853	1.5928	7.7098,	-2	52.9219	14.0334
4.0000	10.0552	5.0138	0.7745	1.4860	1.5931	7.6296,	-2	52.9206	14.0400
4.0683	10.4040	5.1000	0.7741	1.4908	1.5948	7.1501,	-2	52.9124	14.0800
4.1000	10.5676	5.1399	0.7740	1.4930	1.5955	6.9396,	-2	52.9086	14.0978
4.1476	10.8159	5.2000	0.7737	1.4962	1.5966	6.6362,	-2	52.9032	14.1240
4.2000	11.0927	5.2661	0.7735	1.4995	1.5978	6.3193,	-2	52.8974	14.1517
4.2268	11.2358	5.3000	0.7733	1.5012	1.5984	6.1636,	-2	52.8945	14.1655
4.3000	11.6304	5.3922	0.7730	1.5057	1.5999	5.7611,	-2	52.8867	14.2019
4.3061	11.6639	5.4000	0.7730	1.5061	1.6000	5.7287,	-2	52.8861	14.2049
4.3855	12.1000	5.5000	0.7726	1.5108	1.6016	5.3283,	-2	52.8781	14.2422
4.4000	12.1809	5.5184	0.7726	1.5116	1.6019	5.2583,	-2	52.8767	14.2488
4.4647	12.5438	5.6000	0.7723	1.5152	1.6031	4.9597,	-2	52.8704	14.2775
4.5000	12.7441	5.6445	0.7721	1.5171	1.6038	4.8050,	-2	52.8671	14.2927
4.5440	12.9959	5.7000	0.7720	1.5195	1.6046	4.6198,	-2	52.8631	14.3111
4.6000	13.3200	5.7706	0.7718	1.5224	1.6055	4.3959,	-2	52.8581	14.3337
4.6233	13.4560	5.8000	0.7717	1.5236	1.6059	4.3063,	-2	52.8561	14.3429
4.7000	13.9085	5.8967	0.7714	1.5274	1.6072	4.0262,	-2	52.8496	14.3722
4.7026	13.9240	5.9000	0.7714	1.5275	1.6072	4.0170,	-2	52.8494	14.3732
4.7819	14.4000	6.0000	0.7711	1.5313	1.6085	3.7498,	-2	52.8429	14.4020
4.8000	14.5098	6.0228	0.7711	1.5321	1.6088	3.6918,	-2	52.8415	14.4084
4.8612	14.8840	6.1000	0.7709	1.5349	1.6097	3.5029,	-2	52.8367	14.4294
4.9000	15.1237	6.1489	0.7708	1.5366	1.6102	3.3890,	-2	52.8338	14.4424
4.9405	15.3760	6.2000	0.7707	1.5383	1.6108	3.2746,	-2	52.8308	14.4556
5.0000	15.7504	6.2750	0.7705	1.5408	1.6116	3.1145,	-2	52.8265	14.4744
5.0198	15.8759	6.3000	0.7704	1.5417	1.6119	3.0632,	-2	52.8251	14.4805
5.0845	16.2898	6.3816	0.7703	1.5443	1.6127	2.9025,	-2	52.8207	14.5000
5.0991	16.3839	6.4000	0.7702	1.5448	1.6129	2.8675,	-2	52.8197	14.5043
5.1000	16.3897	6.4011	0.7702	1.5449	1.6129	2.8654,	-2	52.8196	14.5045
5.1784	16.8998	6.5000	0.7700	1.5479	1.6139	2.6862,	-2	52.8144	14.5270
5.2000	17.0417	6.5272	0.7700	1.5487	1.6142	2.6391,	-2	52.8130	14.5330
5.2577	17.4240	6.6000	0.7698	1.5509	1.6149	2.5179,	-2	52.8094	14.5487
5.3000	17.7064	6.6533	0.7697	1.5524	1.6154	2.4333,	-2	52.8068	14.5599
5.3371	17.9559	6.7000	0.7696	1.5537	1.6158	2.3618,	-2	52.8045	14.5694
5.4000	18.3837	6.7793	0.7695	1.5559	1.6165	2.2459,	-2	52.8008	14.5853
5.4164	18.4960	6.8000	0.7695	1.5564	1.6167	2.2168,	-2	52.7999	14.5893

TABLE 5—*continued*

5.4957	19.0439	6.9000	0.7693	1.5591	1.6175	2.0821,	-2	52.7954	14.6083
5.5000	19.0738	6.9054	0.7693	1.5592	1.6176	2.0751,	-2	52.7951	14.6093
5.5750	19.6000	7.0000	0.7691	1.5616	1.6183	1.9568,	-2	52.7911	14.6265
5.6000	19.7765	7.0315	0.7691	1.5624	1.6186	1.9192,	-2	52.7897	14.6321
5.6543	20.1638	7.1000	0.7690	1.5640	1.6191	1.8403,	-2	52.7869	14.6440
5.7000	20.4919	7.1575	0.7689	1.5654	1.6195	1.7768,	-2	52.7846	14.6537
5.7337	20.7359	7.2000	0.7688	1.5664	1.6199	1.7317,	-2	52.7829	14.6608
5.8000	21.2200	7.2835	0.7687	1.5683	1.6205	1.6467,	-2	52.7797	14.6742
5.8150	21.3160	7.3000	0.7687	1.5687	1.6206	1.6305,	-2	52.7790	14.6768
5.8924	21.9041	7.4000	0.7686	1.5708	1.6213	1.5362,	-2	52.7753	14.6923
5.9000	21.9608	7.4096	0.7685	1.5710	1.6213	1.5275,	-2	52.7750	14.6937
5.9717	22.4997	7.5000	0.7684	1.5730	1.6219	1.4482,	-2	52.7717	14.7071
6.0000	22.7142	7.5356	0.7684	1.5737	1.6222	1.4183,	-2	52.7705	14.7122
6.0510	23.1038	7.6000	0.7683	1.5750	1.6226	1.3661,	-2	52.7683	14.7214
6.1000	23.4804	7.6617	0.7682	1.5762	1.6230	1.3181,	-2	52.7662	14.7299
6.1304	23.7158	7.7000	0.7682	1.5770	1.6232	1.2893,	-2	52.7649	14.7351
6.2000	24.2592	7.7877	0.7681	1.5786	1.6237	1.2261,	-2	52.7621	14.7467
6.2097	24.3358	7.8000	0.7681	1.5789	1.6238	1.2176,	-2	52.7617	14.7483
6.2891	24.9637	7.9000	0.7680	1.5807	1.6244	1.1505,	-2	52.7586	14.7610
6.3000	25.0506	7.9137	0.7679	1.5809	1.6244	1.1416,	-2	52.7582	14.7627
6.3685	25.6001	8.0000	0.7678	1.5825	1.6249	1.0876,	-2	52.7556	14.7732
6.4000	25.8548	8.0397	0.7678	1.5831	1.6251	1.0638,	-2	52.7544	14.7779
6.4478	26.2440	8.1000	0.7677	1.5842	1.6254	1.0288,	-2	52.7527	14.7850
6.5000	26.6716	8.1657	0.7677	1.5853	1.6258	9.9223,	-3	52.7508	14.7925
6.5272	26.8960	8.2000	0.7676	1.5858	1.6260	9.7374,	-3	52.7498	14.7964
6.6000	27.5011	8.2917	0.7676	1.5873	1.6264	9.2621,	-3	52.7473	14.8064
6.6065	27.5559	8.3000	0.7676	1.5874	1.6265	9.2207,	-3	52.7471	14.8073
6.6859	28.2238	8.4000	0.7675	1.5890	1.6269	8.7361,	-3	52.7445	14.8179
6.7000	28.3433	8.4177	0.7674	1.5893	1.6270	8.6531,	-3	52.7440	14.8197
6.7653	28.9001	8.5000	0.7674	1.5905	1.6274	8.2808,	-3	52.7419	14.8281
6.8000	29.1981	8.5437	0.7673	1.5911	1.6276	8.0907,	-3	52.7409	14.8325
6.8446	29.5839	8.6000	0.7673	1.5919	1.6279	7.8536,	-3	52.7395	14.8380
6.9000	30.0656	8.6697	0.7672	1.5929	1.6282	7.5709,	-3	52.7378	14.8446
6.9240	30.2757	8.7000	0.7672	1.5934	1.6283	7.4520,	-3	52.7371	14.8475
7.0000	30.9458	8.7957	0.7671	1.5947	1.6287	7.0900,	-3	52.7349	14.8563
7.0034	30.9760	8.8000	0.7671	1.5947	1.6287	7.0743,	-3	52.7348	14.8567
7.0828	31.6838	8.9000	0.7670	1.5960	1.6291	6.7191,	-3	52.7325	14.8656
7.1000	31.8387	8.9217	0.7670	1.5963	1.6292	6.6447,	-3	52.7321	14.8675
7.1621	32.4000	9.0000	0.7670	1.5973	1.6295	6.3846,	-3	52.7304	14.8742
7.2000	32.7442	9.0477	0.7669	1.5979	1.6297	6.2321,	-3	52.7294	14.8782
7.2415	33.1237	9.1000	0.7669	1.5986	1.6299	6.0698,	-3	52.7283	14.8825
7.3000	33.6624	9.1737	0.7669	1.5995	1.6302	5.8494,	-3	52.7268	14.8885
7.3209	33.8559	9.2000	0.7668	1.5998	1.6303	5.7729,	-3	52.7262	14.8906
7.4000	34.5933	9.2996	0.7668	1.6010	1.6306	5.4941,	-3	52.7242	14.8983
7.4003	34.5957	9.3000	0.7668	1.6010	1.6306	5.4933,	-3	52.7242	14.8984
7.4796	35.3438	9.4000	0.7667	1.6021	1.6310	5.2293,	-3	52.7223	14.9059
7.5000	35.5369	9.4256	0.7667	1.6024	1.6311	5.1641,	-3	52.7218	14.9078
7.5590	36.1000	9.5000	0.7666	1.6032	1.6313	4.9802,	-3	52.7205	14.9132
7.6000	36.4931	9.5516	0.7666	1.6038	1.6315	4.8573,	-3	52.7195	14.9169
7.6384	36.8636	9.6000	0.7666	1.6043	1.6316	4.7452,	-3	52.7186	14.9203
7.7000	37.4620	9.6775	0.7665	1.6051	1.6319	4.5718,	-3	52.7173	14.9257
7.7178	37.6358	9.7000	0.7665	1.6053	1.6319	4.5231,	-3	52.7169	14.9272
7.7972	38.4159	9.8000	0.7665	1.6063	1.6323	4.3131,	-3	52.7152	14.9339
7.8000	38.4435	9.8035	0.7665	1.6064	1.6323	4.3059,	-3	52.7151	14.9341
7.8766	39.2040	9.9000	0.7664	1.6073	1.6326	4.1146,	-3	52.7135	14.9404
7.9000	39.4378	9.9295	0.7664	1.6076	1.6326	4.0582,	-3	52.7130	14.9422
7.9560	40.0001	10.0000	0.7664	1.6083	1.6328	3.9268,	-3	52.7119	14.9466
8.0000	40.4447	10.0554	0.7663	1.6088	1.6330	3.8271,	-3	52.7110	14.9500

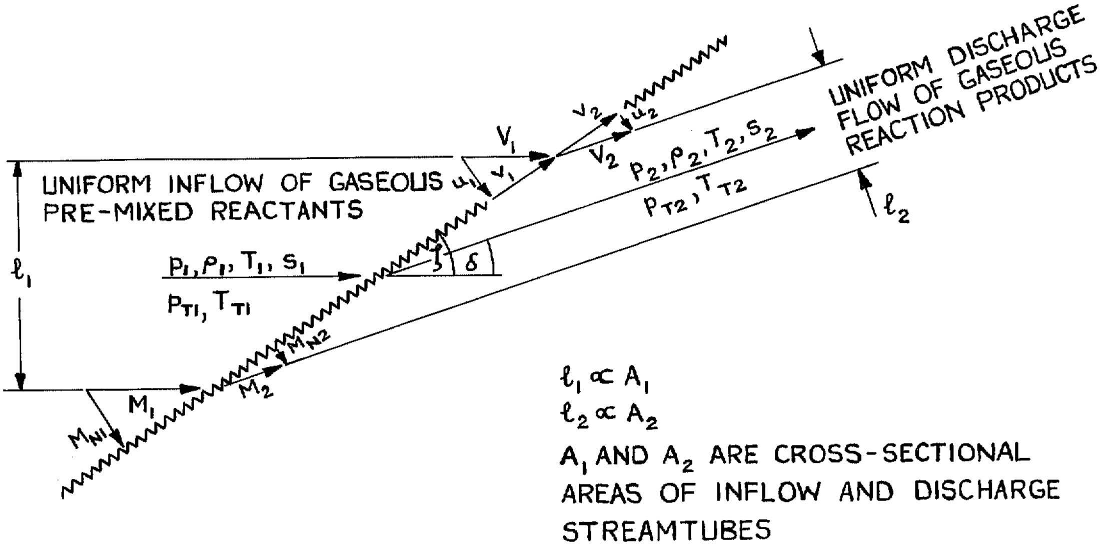

FIG. 1a. Basic flow model.

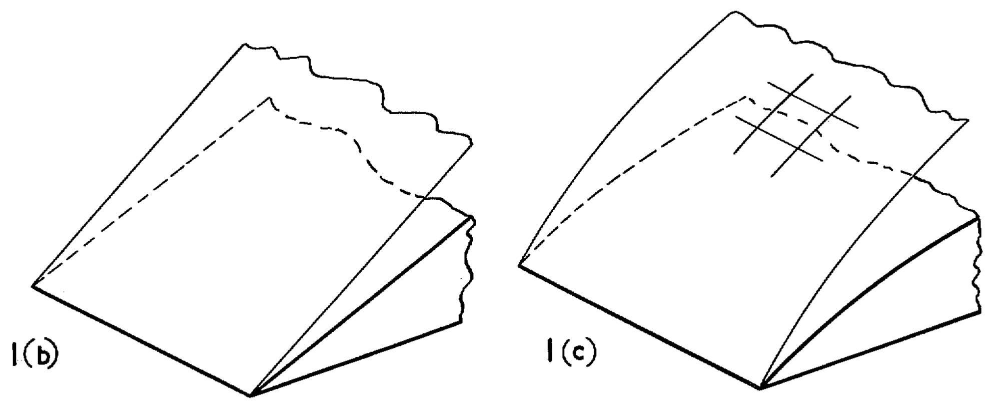

FIG. 1b, 1c. Two-dimensional waves.

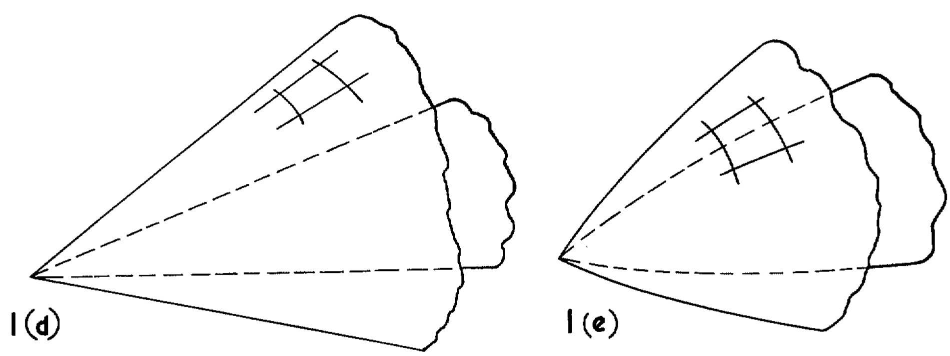

FIG. 1d, 1e. Axisymmetric waves.

FIG. 1. Flow models.

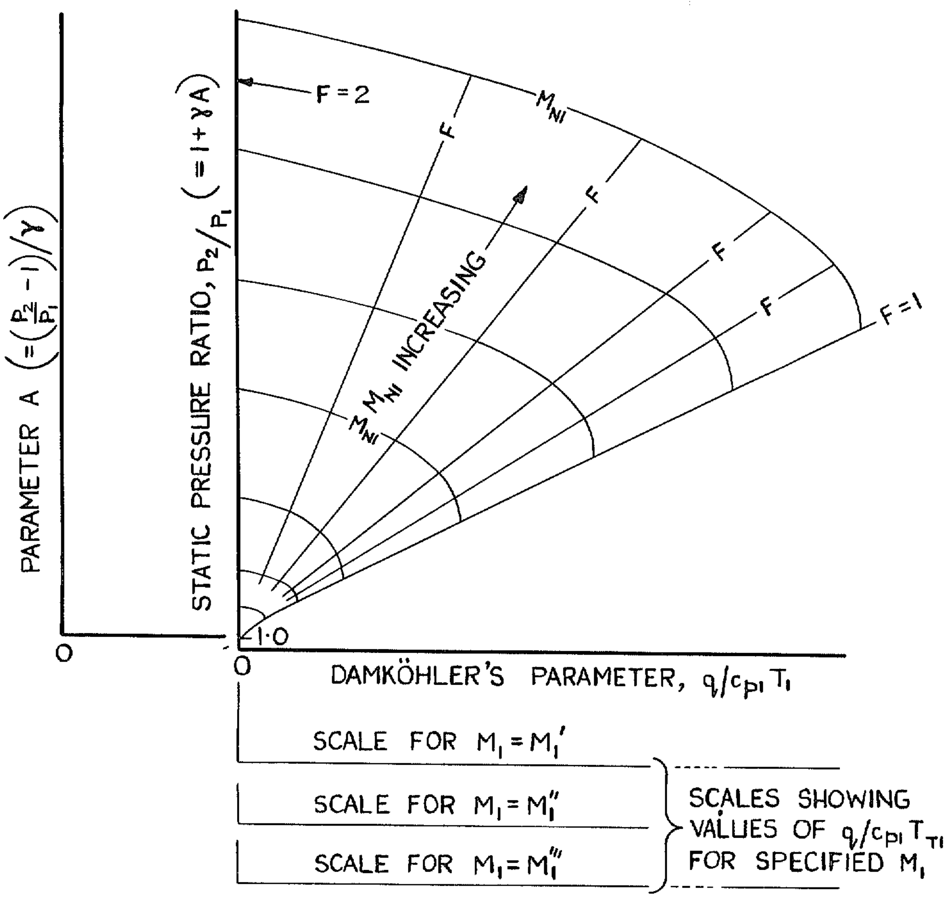

FIG. 2. Variation of static-pressure ratio and parameter A with $q/c_{p1}\,T_1$, F and M_{N1}.

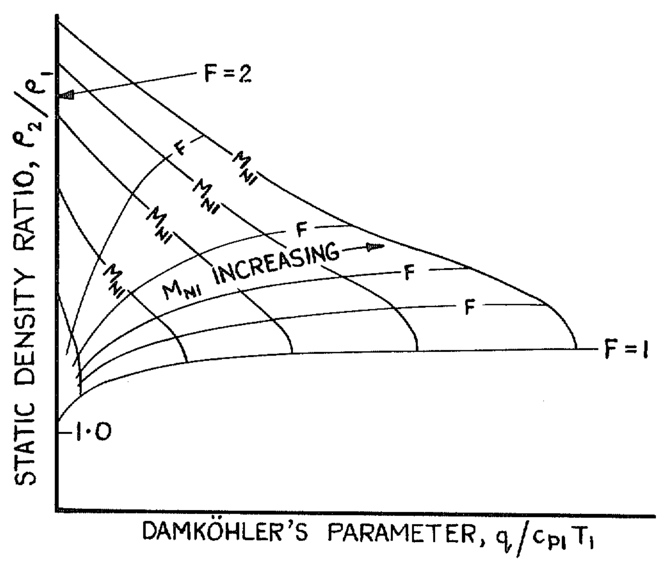

FIG. 3. Variation of static-density ratio with $q/c_{p1}\,T_1$, F and M_{N1}.

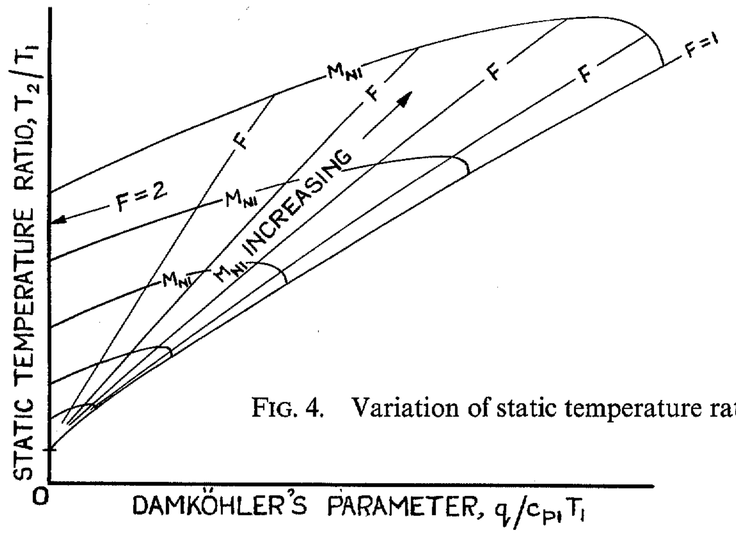

FIG. 4. Variation of static temperature ratio with $q/c_{p1}\,T_1$, F and M_{N1}.

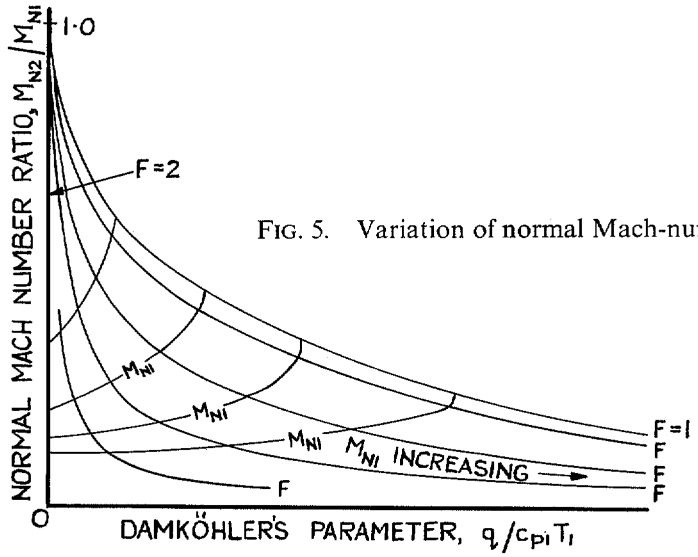

FIG. 5. Variation of normal Mach-number ratio with $q/c_{p1}\,T_1$, F and M_{N1}.

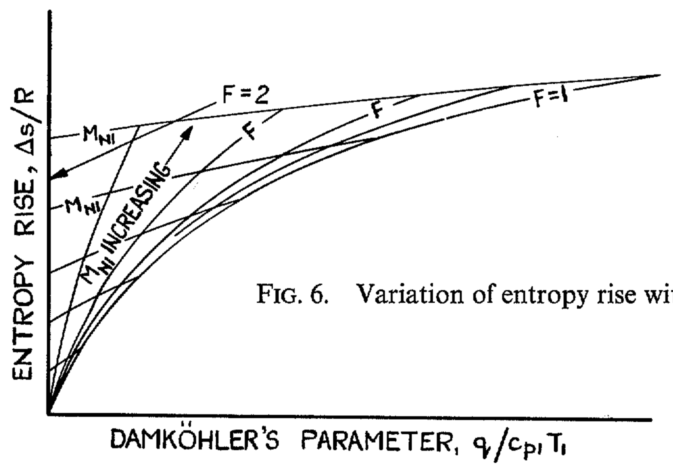

FIG. 6. Variation of entropy rise with $q/c_{p1}\,T_1$, F and M_{N1}.

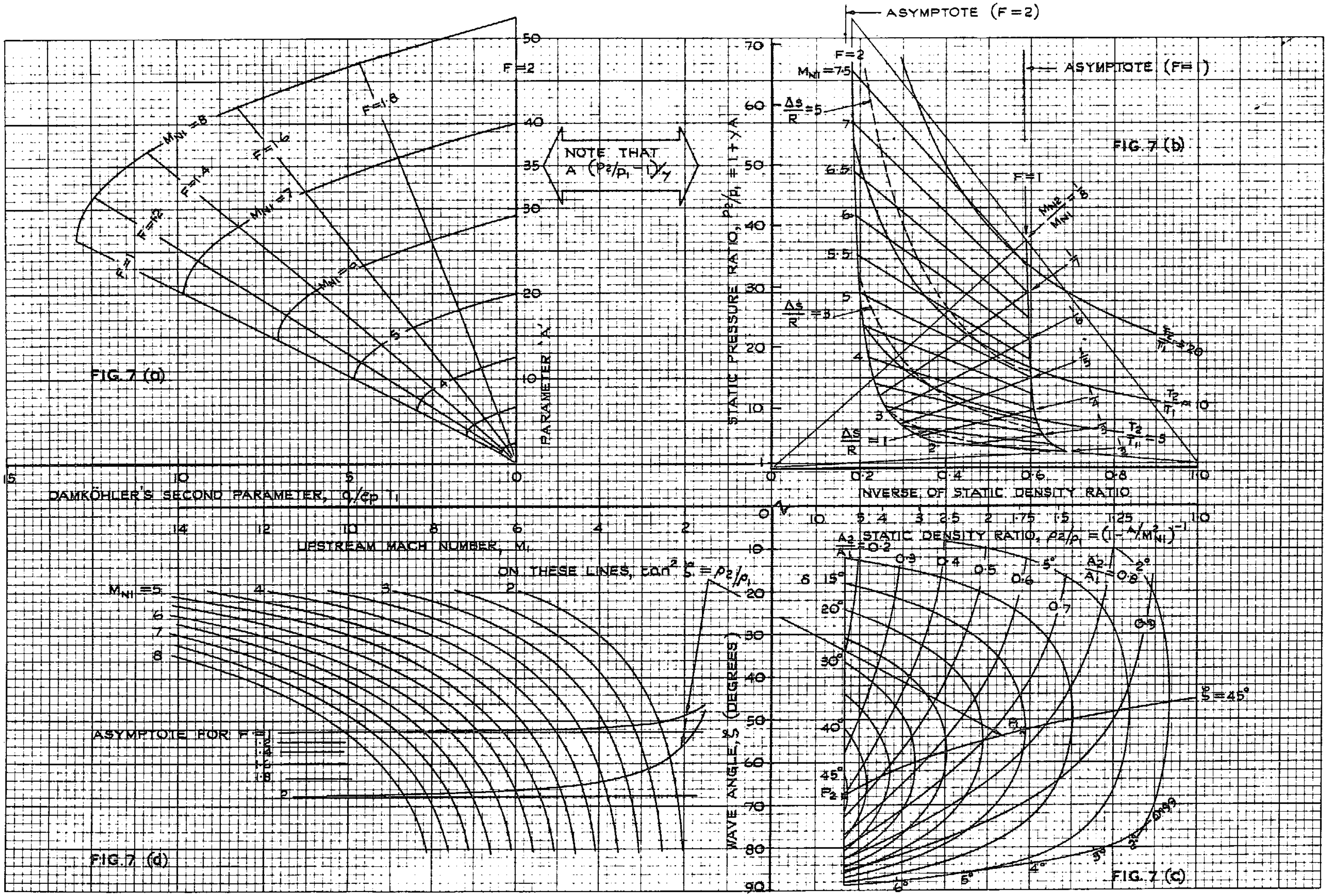

FIG. 7. Compound chart for shock and detonation waves ($\gamma = 1{\cdot}4$, $1 \leqslant F \leqslant 2$).

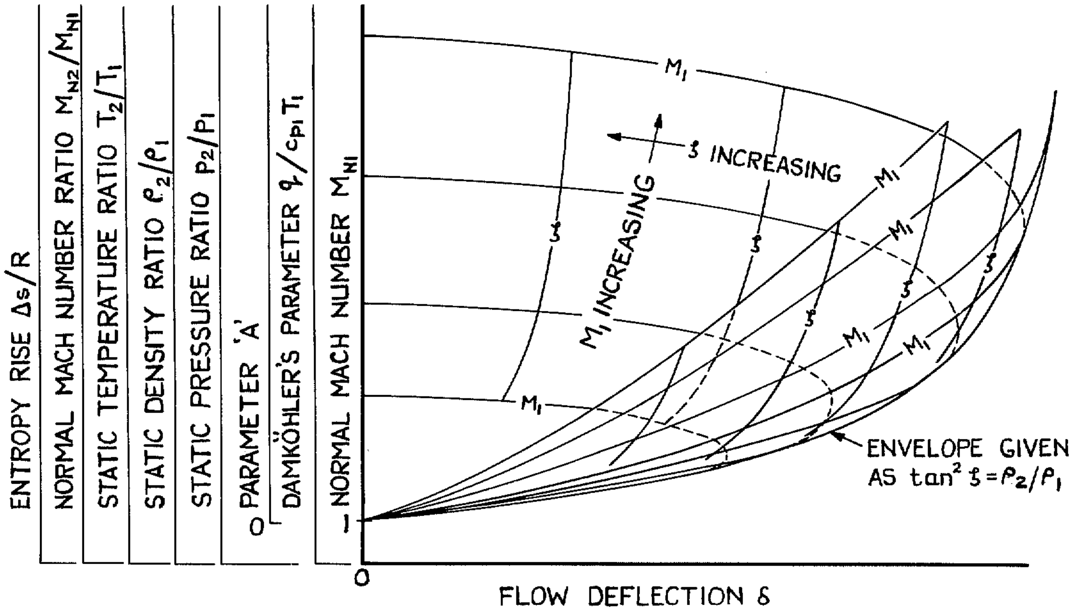

FIG. 8. Variation of normal Mach number (and dependent functions) with δ, ζ and M_1, for waves of given F ($1 \leqslant F \leqslant 2$).

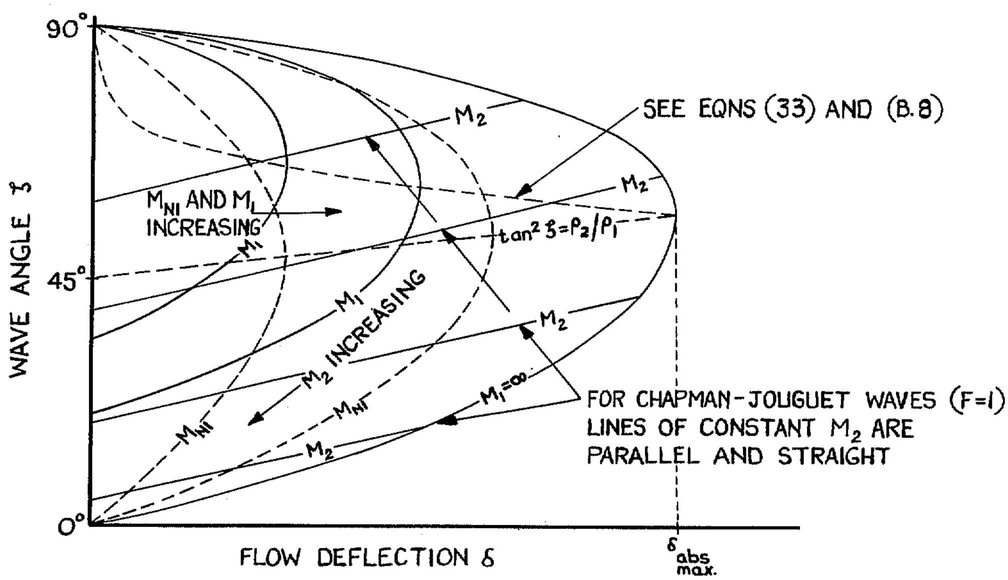

FIG. 9. Variation of wave angle with δ, M_{N1}, M_1 and M_2, for waves of given F ($1 \leqslant F \leqslant 2$).

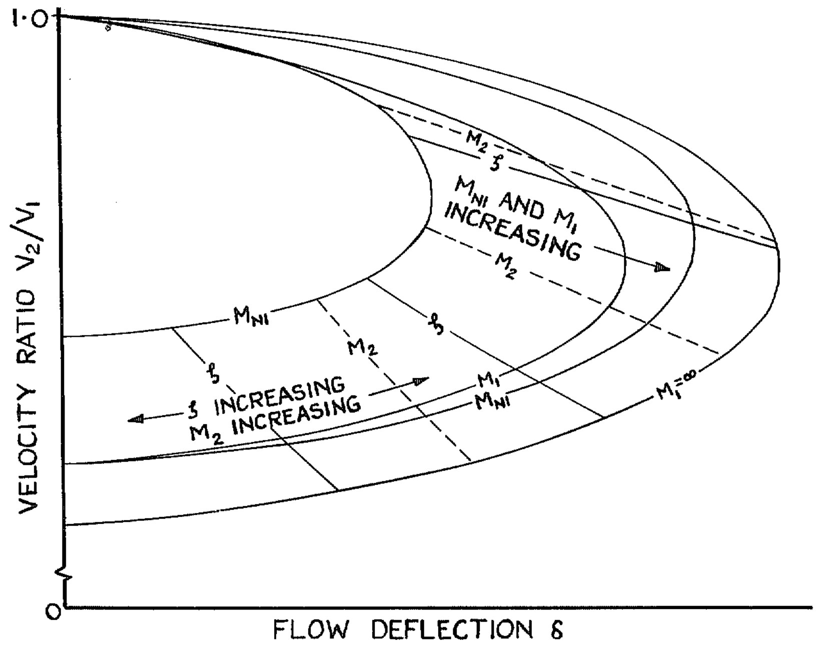

FIG. 10. Variation of velocity ratio with $\delta, \zeta, M_{N1}, M_1$ and M_2, for waves of given F ($1 \leqslant F \leqslant 2$).

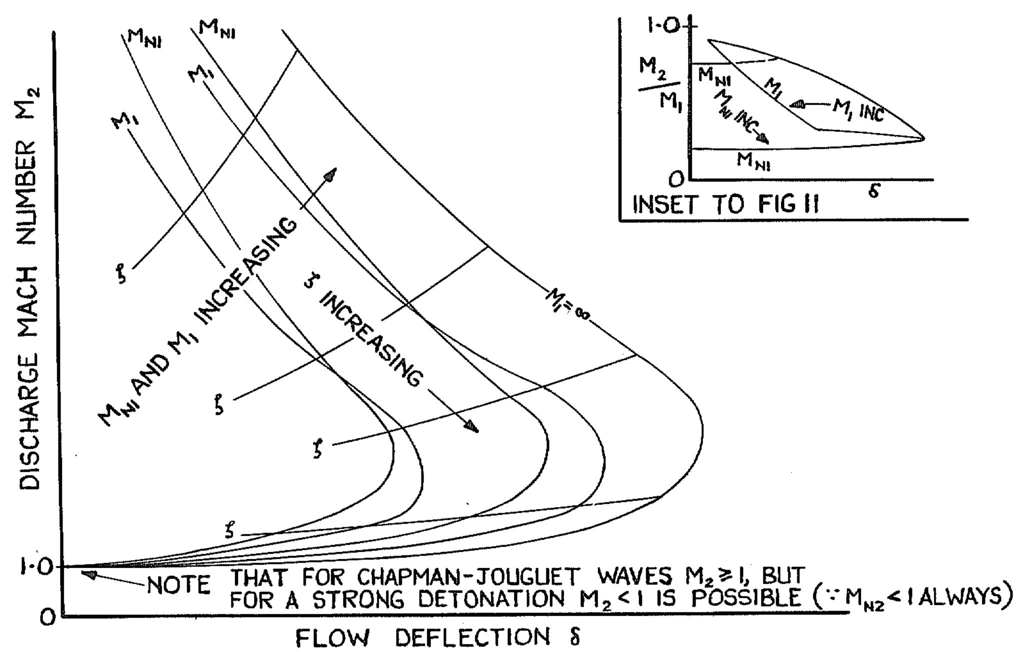

FIG. 11. Variation of discharge Mach number with δ, ζ, M_{N1} and M_1, for waves of given F ($1 \leqslant F \leqslant 2$).

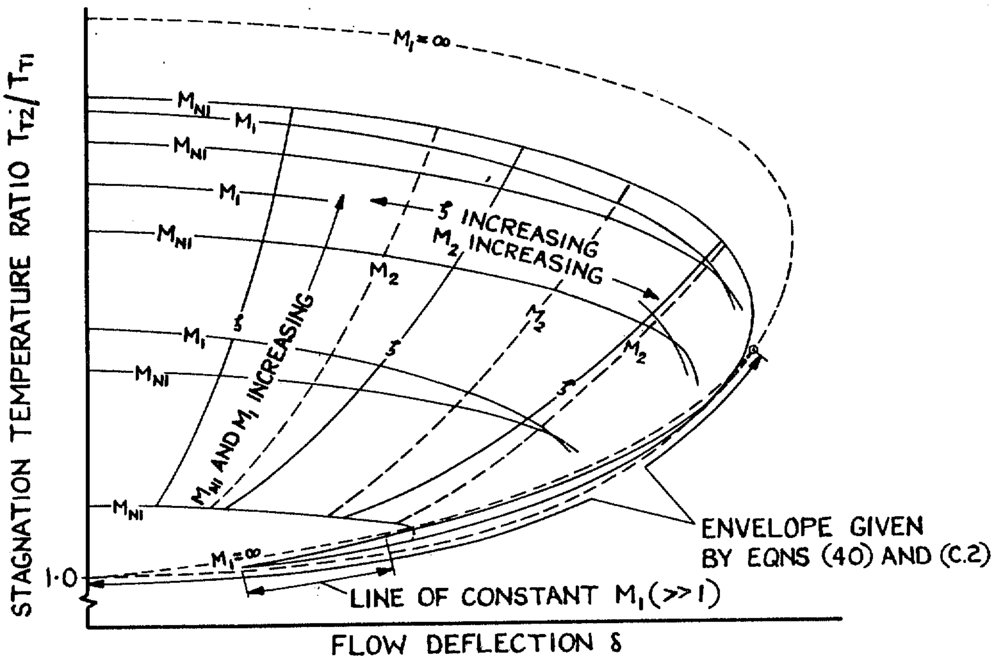

FIG. 12. Variation of stagnation temperature ratio with δ, ζ, M_{N1}, M_1 and M_2, for waves of given F $(1 \leqslant F \leqslant 2)$.

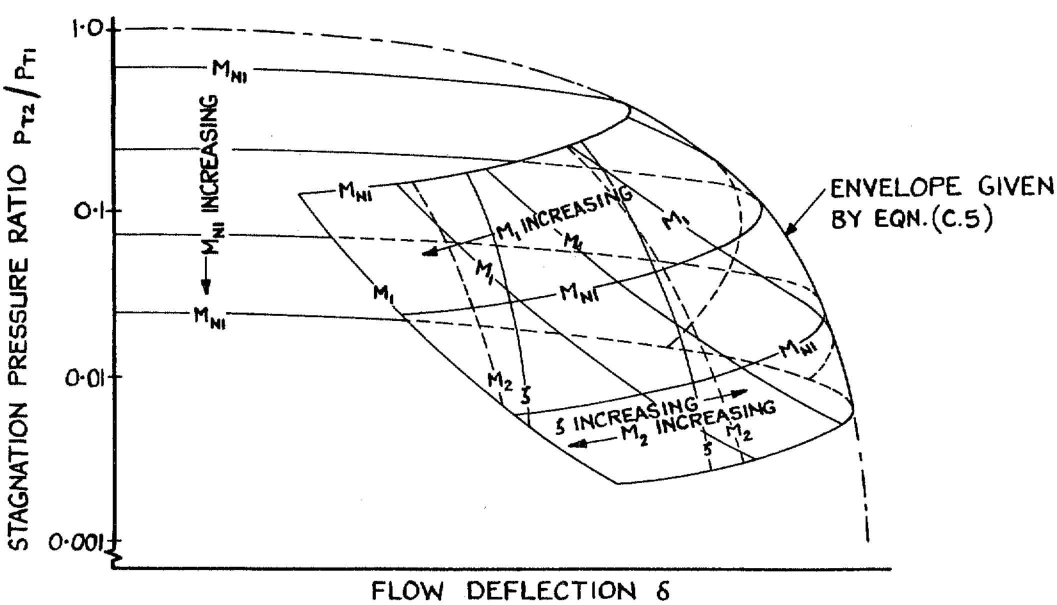

FIG. 13. Variation of stagnation pressure ratio with δ, ζ, M_{N1}, M_1 and M_2, for waves of given F $(1 \leqslant F \leqslant 2)$.

Printed in Wales for Her Majesty's Stationery Office by Allens Printers (Wales) Limited

Dd. 501372 K.5

Printed and published by
HER MAJESTY'S STATIONERY OFFICE

To be purchased from
49 High Holborn, London WC1
13a Castle Street, Edinburgh EH2 3AR
109 St Mary Street, Cardiff CF1 1JW
Brazennose Street, Manchester M60 8AS
50 Fairfax Street, Bristol BS1 3DE
258 Broad Street, Birmingham 1
7 Linenhall Street, Belfast BT2 8AY
or through any bookseller

R. & M. No. 3638
SBN 11 470338 8